

UNIVERSITY OF TWENTE.

MESA+

INSTITUTE FOR NANOTECHNOLOGY

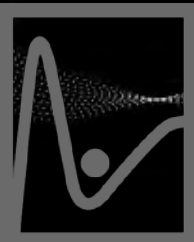
High-frequency surface acoustic waves for acousto-electronic transport



Wilfred G. van der Wiel

NanoElectronics Group, MESA+ Institute for Nanotechnology, University of Twente

SPICE-Workshop Quantum Acoustics, May 18th 2016



SAWtrain
network



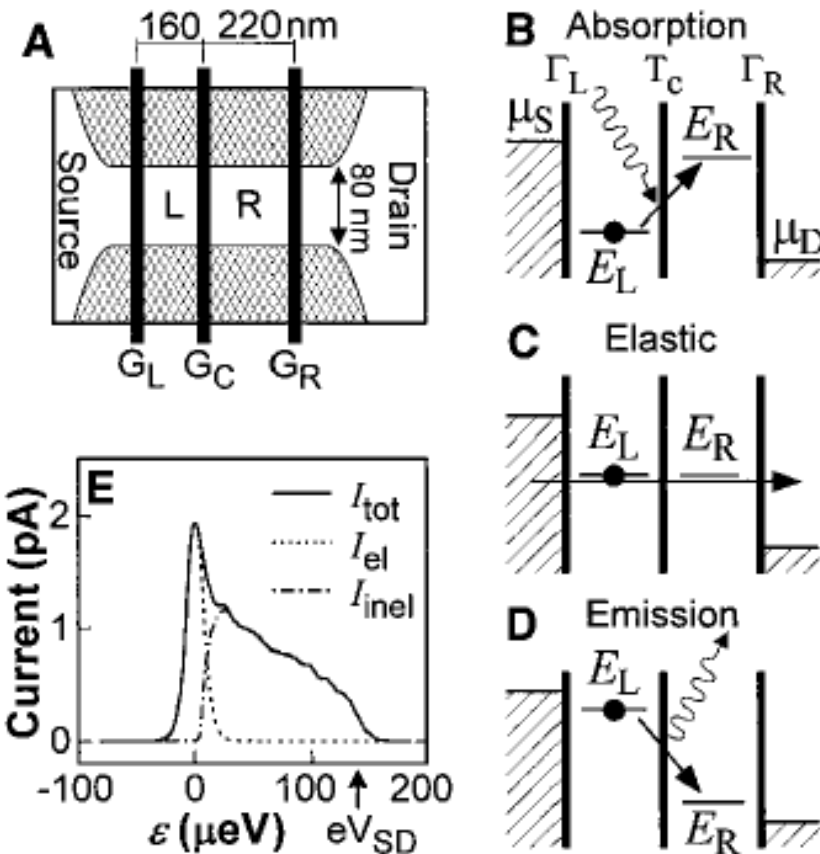
NANO**E**LECTRONICS.



Spontaneous Emission Spectrum in Double Quantum Dot Devices

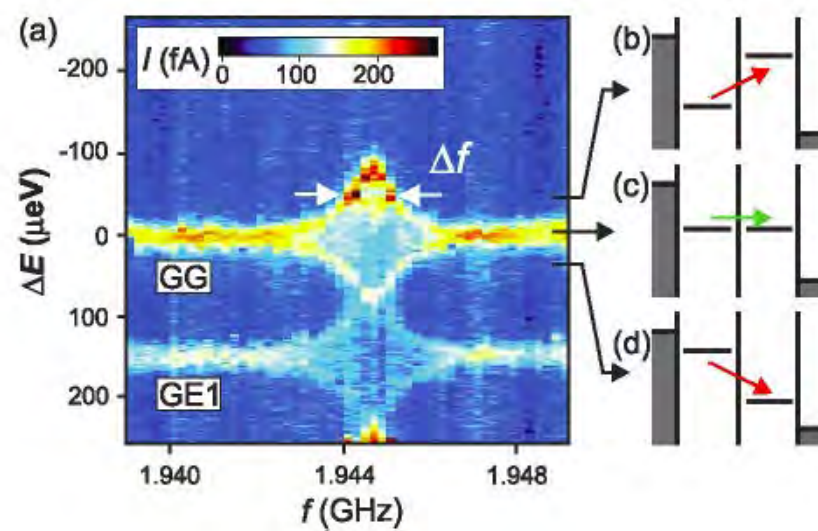
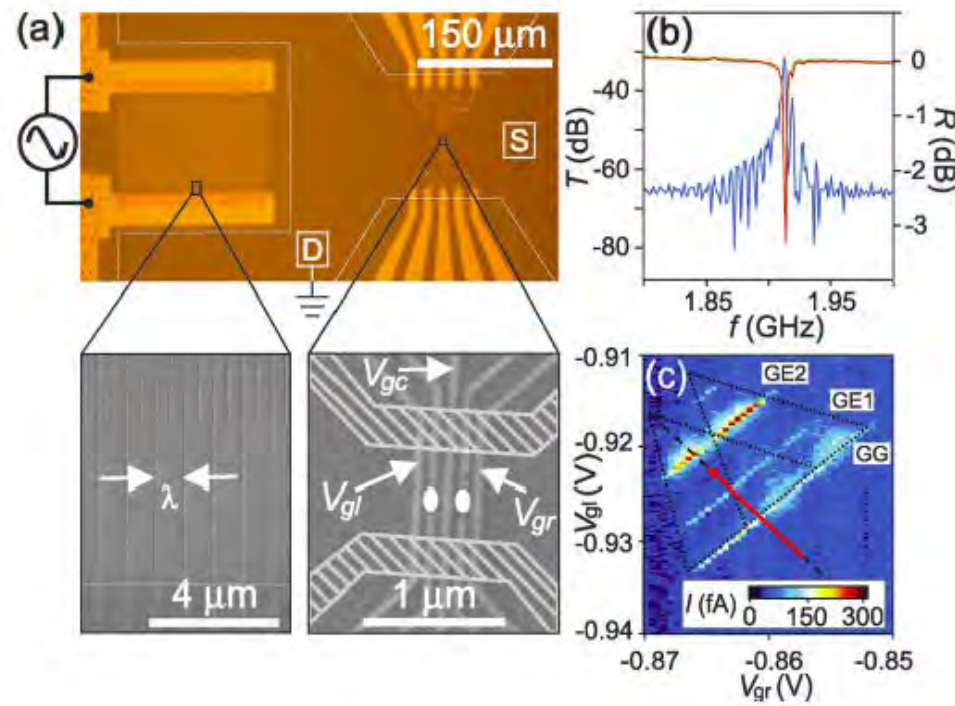
Toshimasa Fujisawa, Tjerk H. Oosterkamp,
Wilfred G. van der Wiel, Benno W. Broer, Ramón Aguado,
Seigo Tarucha, Leo P. Kouwenhoven*

A double quantum dot device is a tunable two-level system for electronic energy states. A dc electron current was used to directly measure the rates for elastic and inelastic transitions between the two levels. For inelastic transitions, energy is exchanged with bosonic degrees of freedom in the environment. The inelastic transition rates are well described by the Einstein coefficients, relating absorption with stimulated and spontaneous emission. The most effectively coupled bosons in the specific environment of the semiconductor device used here were acoustic phonons. The experiments demonstrate the importance of vacuum fluctuations in the environment for quantum dot devices and potential design constraints for their use for preparing long-lived quantum states.



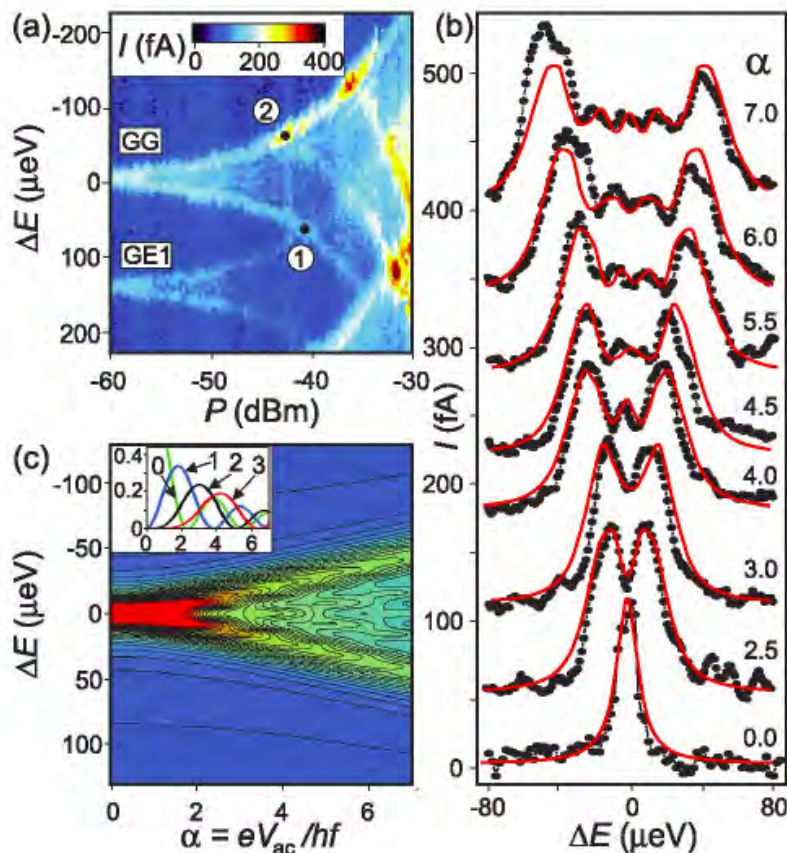
Surface-Acoustic-Wave-Induced Transport in a Double Quantum Dot

W. J. M. Naber,^{1,2,3} T. Fujisawa,^{2,4} H. W. Liu,^{2,5} and W. G. van der Wiel^{1,6}



Surface-Acoustic-Wave-Induced Transport in a Double Quantum Dot

W. J. M. Naber,^{1,2,3} T. Fujisawa,^{2,4} H. W. Liu,^{2,5} and W. G. van der Wiel^{1,6}



Resonance at 1.9446 GHz

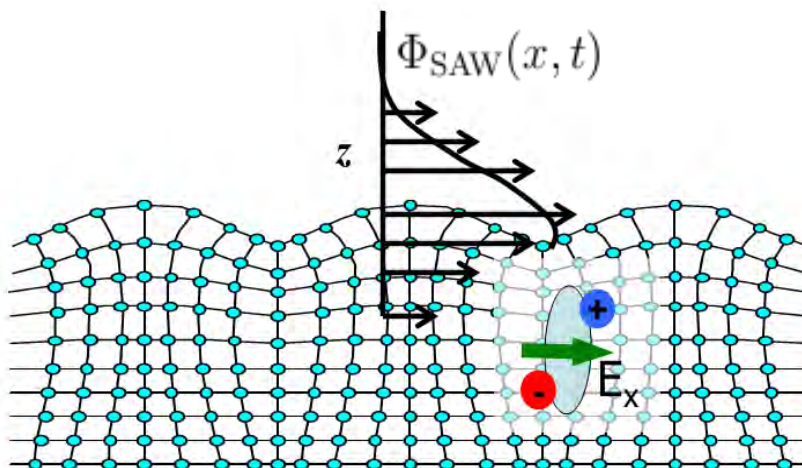
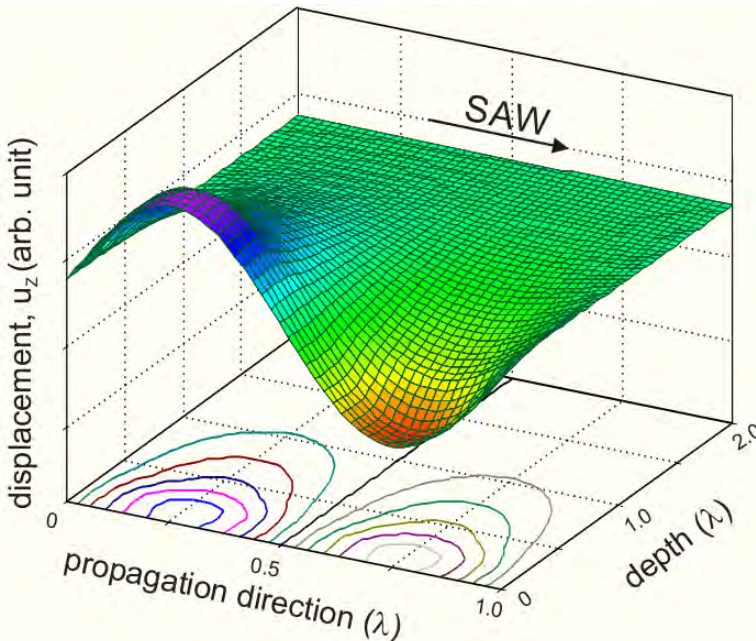
$$hf_{SAW} = 8 \text{ } \mu\text{eV}$$

< GG line width (14 μeV)

→ need for higher frequency

$$\hbar f_{\text{SAW}} \gg k_{\text{B}} T$$

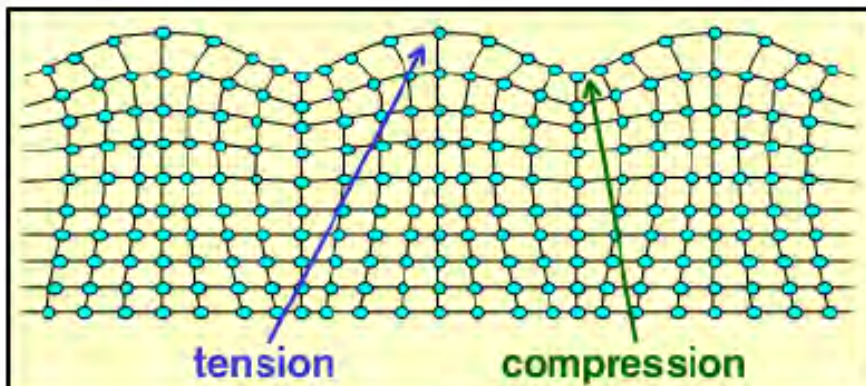
Surface Acoustic Waves (SAWs)



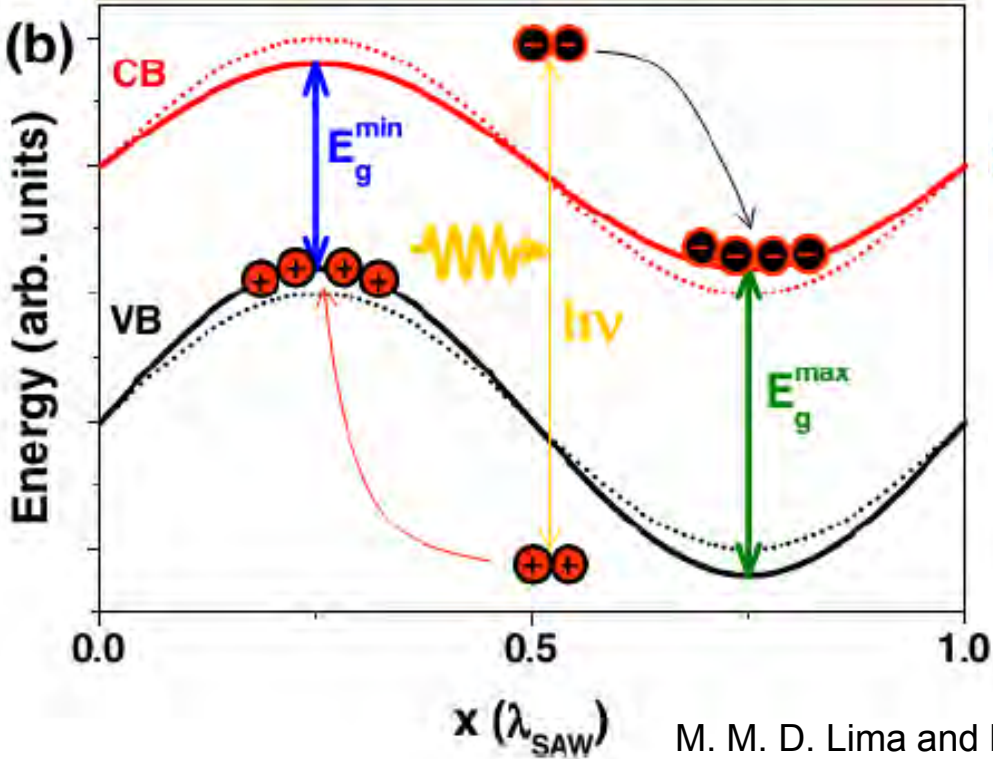
- Mechanical Wave: Rayleigh Wave
longitudinal and transverse motion
- Propagate in the surface with sound velocity
energy concentrated in a thin layer ($\sim \lambda$)
- Small amplitude
less than 1 nm
- Much lower velocity than electromagnetic
waves with a few km/s (EMW:SAW $\sim 1:10^5$)
- Sub-micron wave length

Surface Acoustic Waves (SAWs)

(a)



(b)



Lattice displacement induced
by Rayleigh wave

↓
spatially- and time-
dependent local strain

$$\tilde{\varepsilon}(\mathbf{r}, t)$$

Band-gap modulation
~ meV



Type-I

Piezo-field modulation
~ 100 meV



Type-II

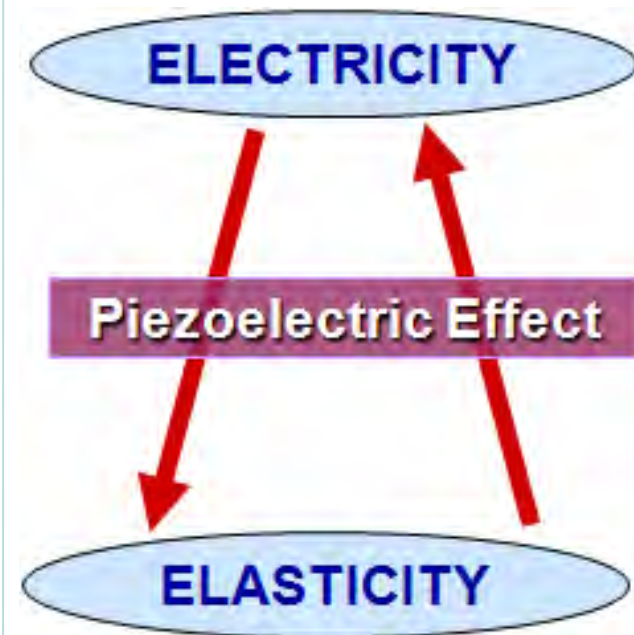
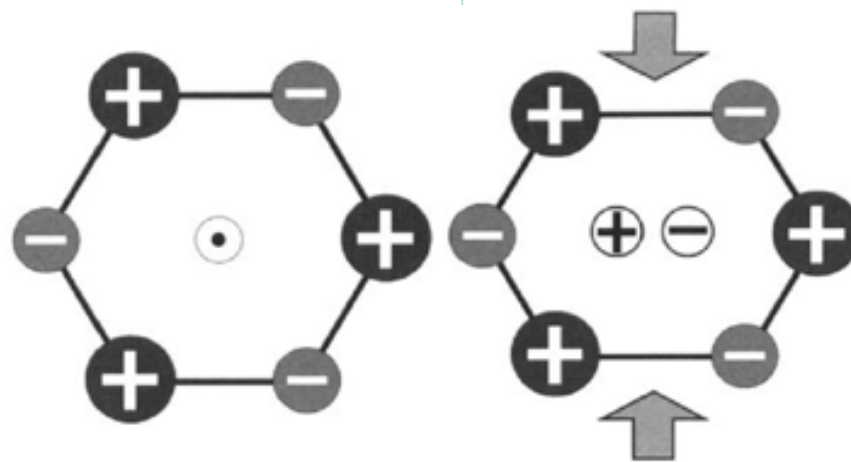
© H. Sanada (NTT BRL)

M. M. D. Lima and P. V. Santos, Rep. Prog.
Phys. **68** 1639 (2005).

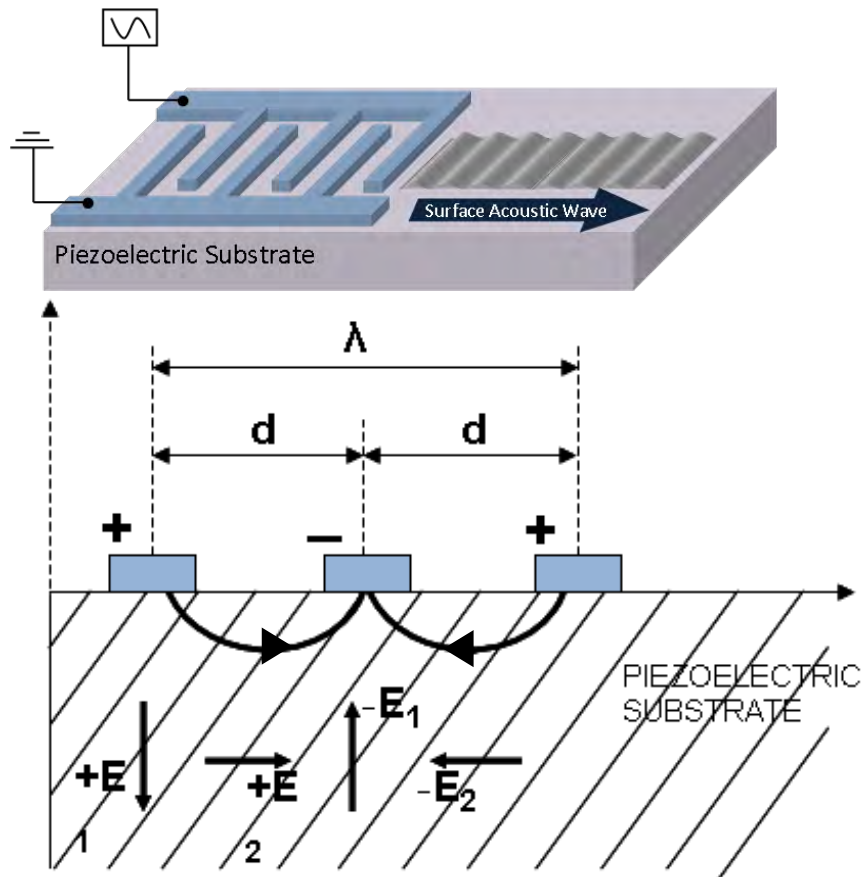
SAWs: Piezoelectricity

The direct piezoelectric effect - the production of electricity when stress is applied

The converse piezoelectric effect - the production of stress and/or strain when an electric field is applied



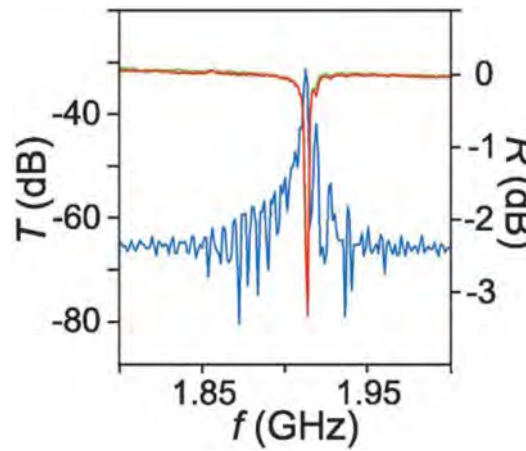
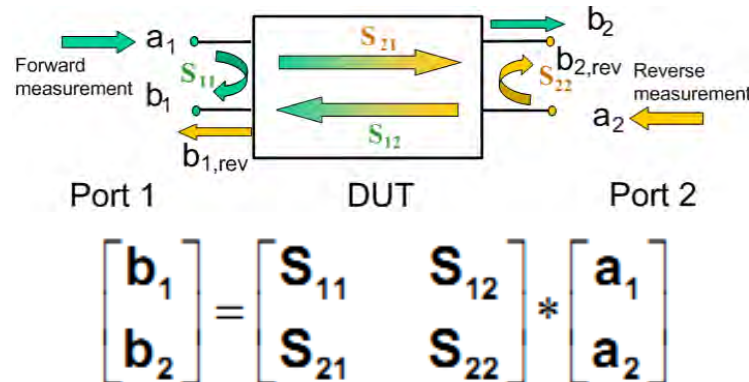
Interdigital Transducers (IDTs)



$$f_{SAW} = v_{SAW} / \lambda_{SAW}$$

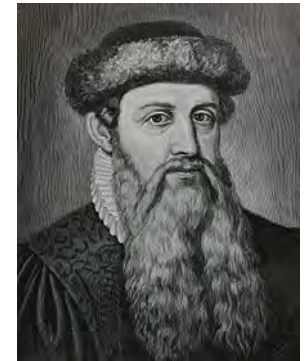
High frequency \equiv narrow fingers

S-parameters describe how the DUT modifies a signal that is transmitted or reflected in forward or reverse direction



W. J. M. Naber et al. PRL 96, 136807 (2006)

Why printing?!



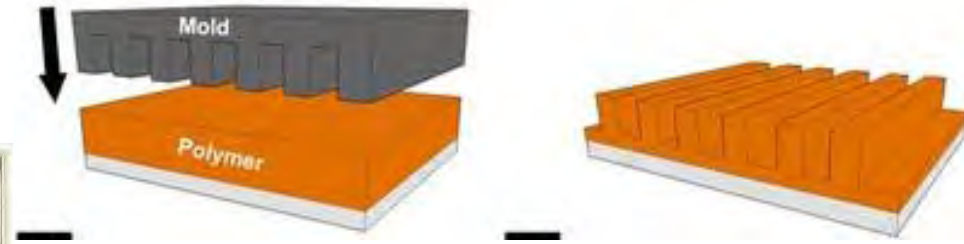
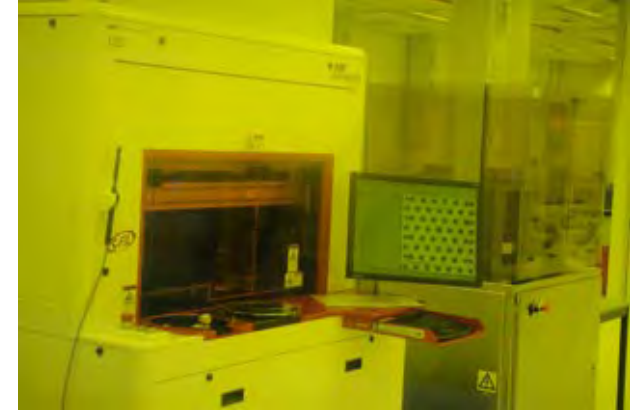
Johannes
Gutenberg
(1440)



Nanoimprint Lithography (NIL)



Stephen
Chou (1996)

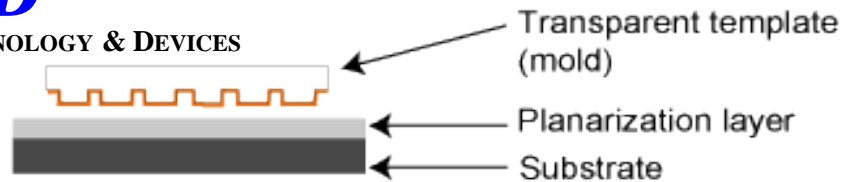


- Fast
- Economical
- Reproducible

UV based Nanoimprint Lithography (UV-NIL)

NT&D

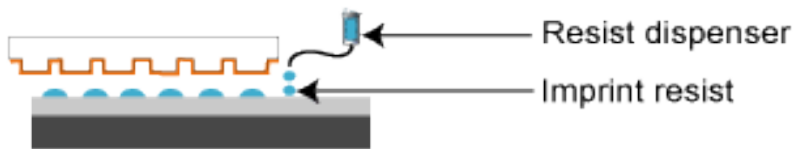
NANOTECHNOLOGY & DEVICES



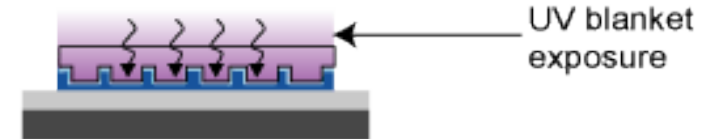
Dr. Boris Vratzov



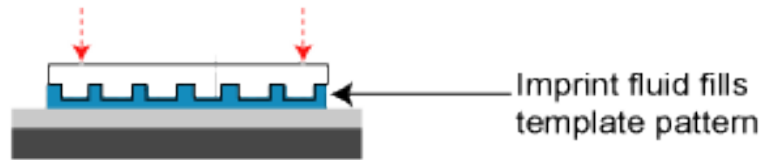
Step 1: Orient template and substrate



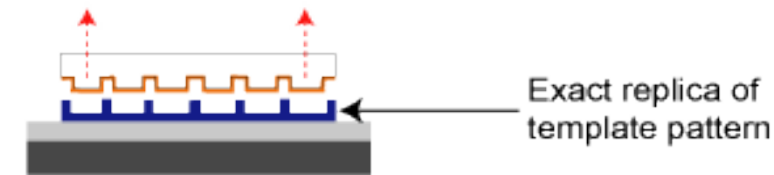
Step 2: Dispense drops of liquid imprint resist



Step 4: Polymerize imprint fluid with UV exposure



Step 3: Lower template and fill pattern



Step 5: Separate template from substrate

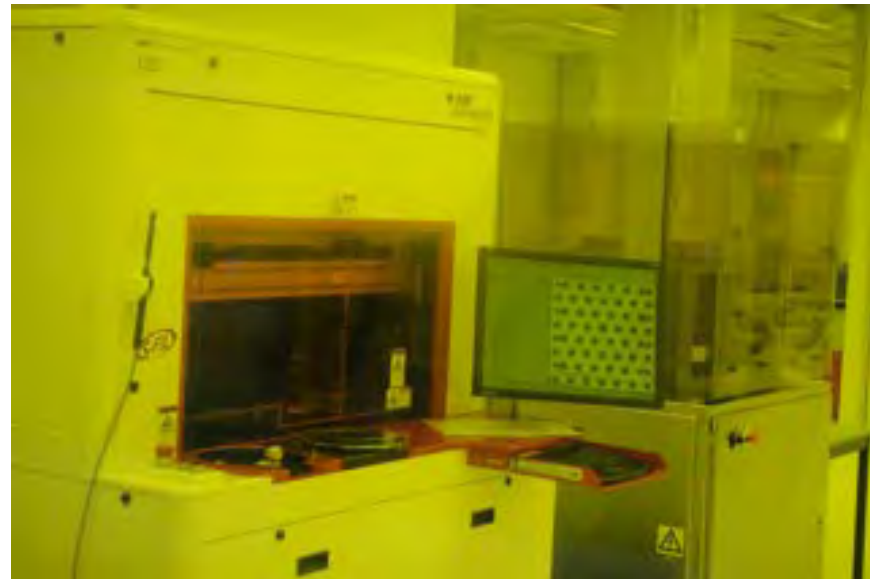
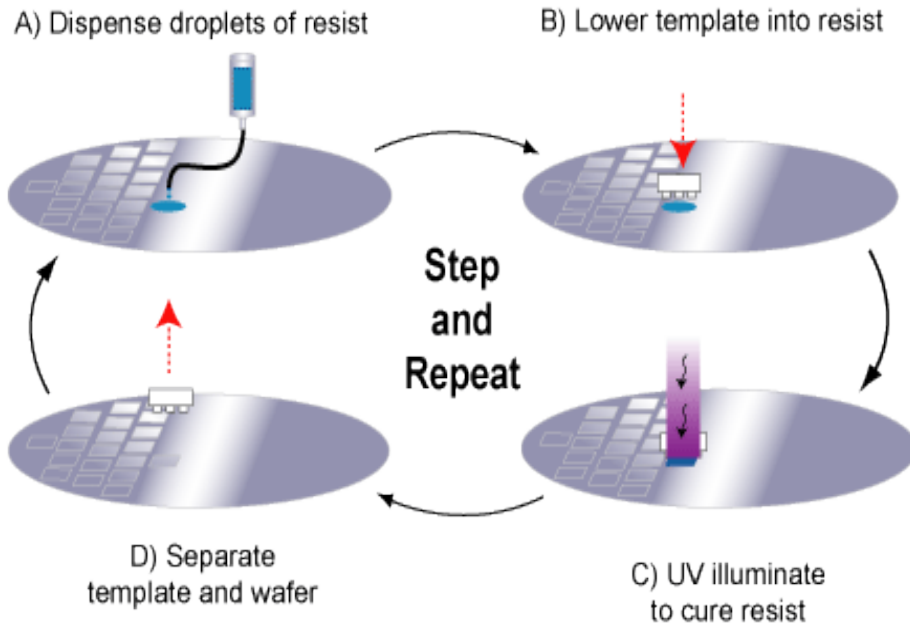
Molecular Imprints, Inc.

- ▶ Low force, room temperature process
- ▶ Precise 2D and 3D nano pattern definition
- ▶ Resist deposition by nano dispensing techniques
- ▶ Ultra high degree of uniformity and reproducibility
- ▶ Complete design definition
- ▶ Step & repeat on wafer scale

MESA+

INSTITUTE FOR NANOTECHNOLOGY

UV based Nanoimprint Lithography (UV-NIL)



200mm wafer



100mm wafer

UV-NIL: IDT Templates

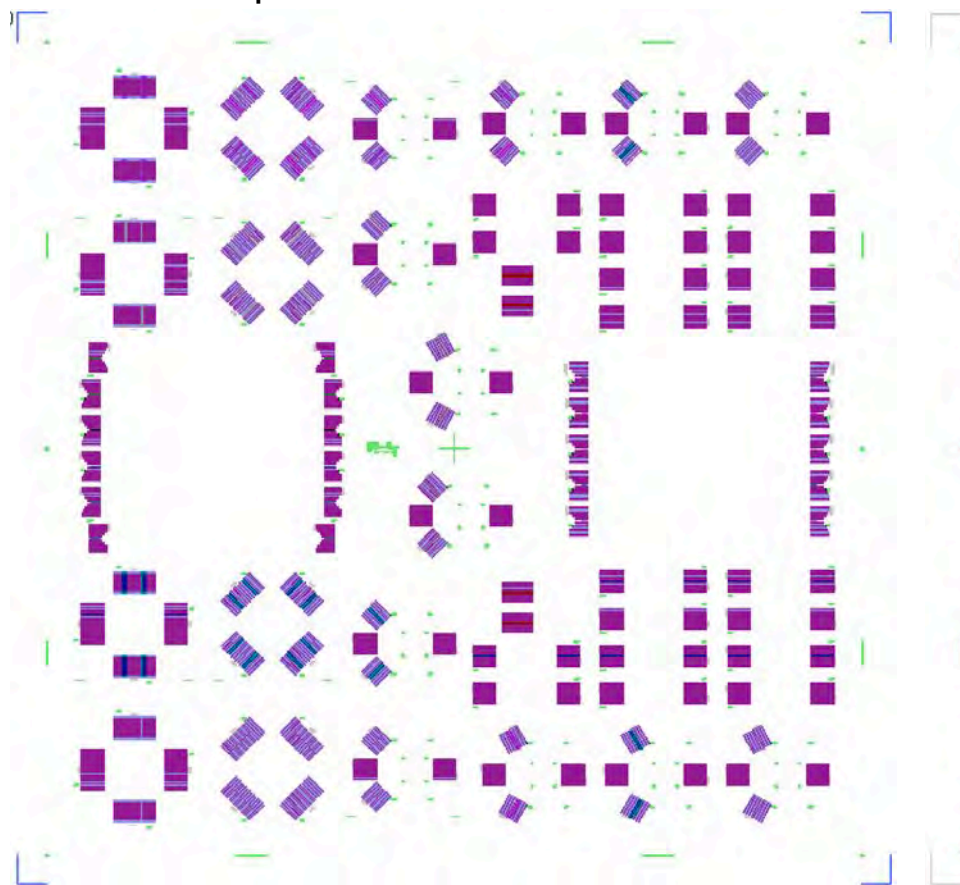
Design in collaboration with Paulo Santos (PDI)

Serkan
Büyükköse



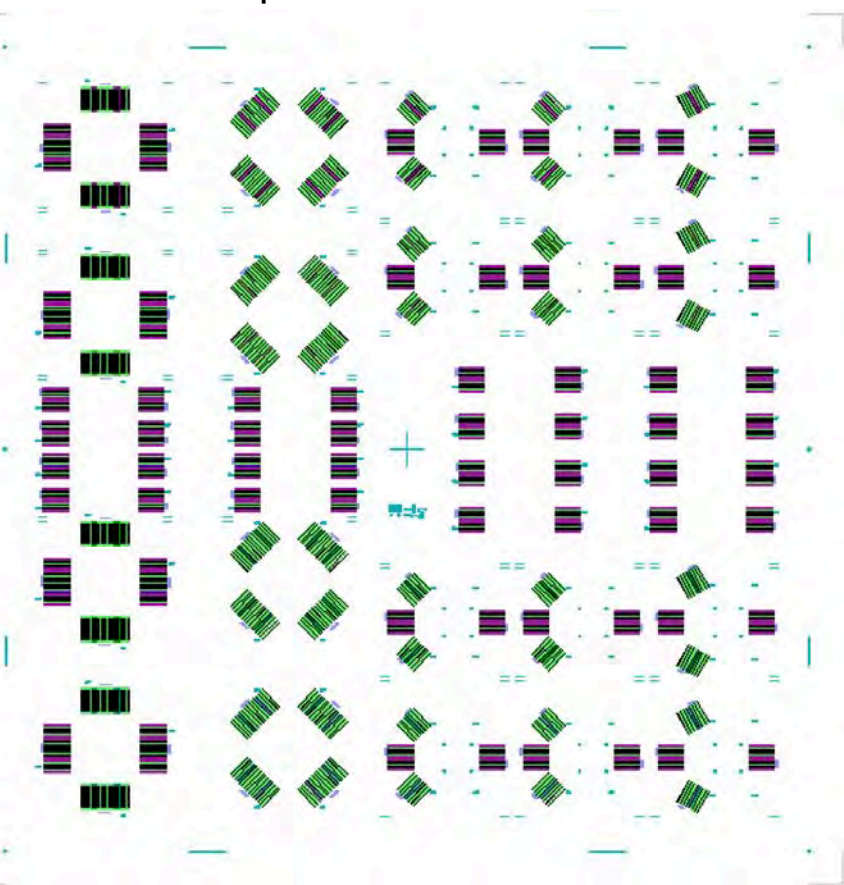
Single Finger Design

Chip size: 13 mm x 13 mm



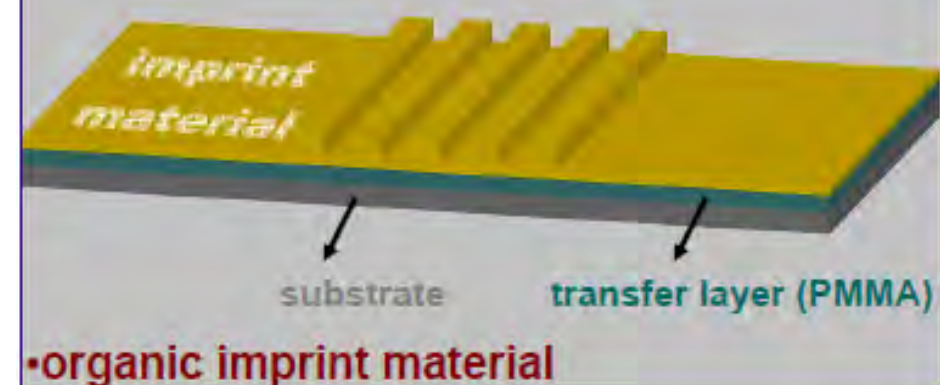
Double Finger Design

Chip size: 13 mm x 13 mm

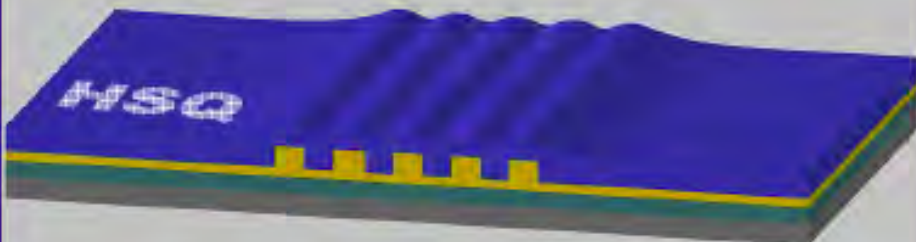


NIL of Interdigitated transducers (SFIL-R)

1 Pattern definition by SFIL method

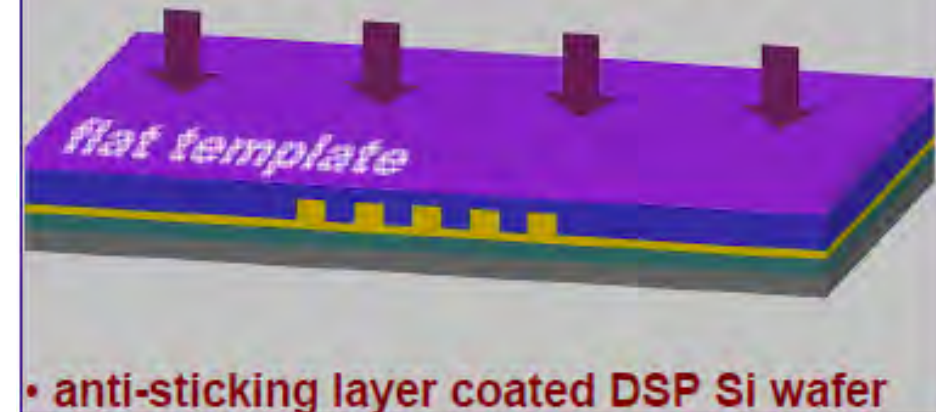


2 HSQ application by Spin Coating

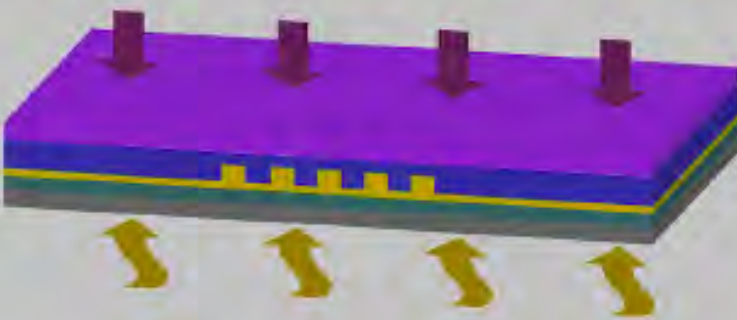


- shows deformation capability
- acts as etch mask under O₂ plasma

3 Force application with flat stamp



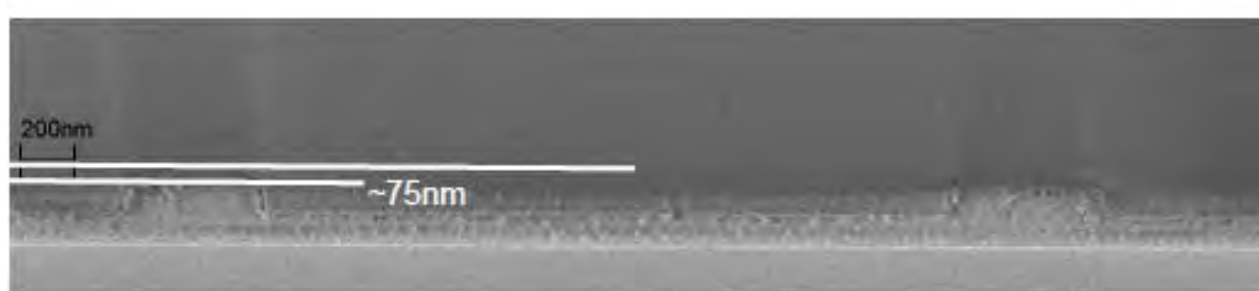
4 Heating up HSQ under the pressure



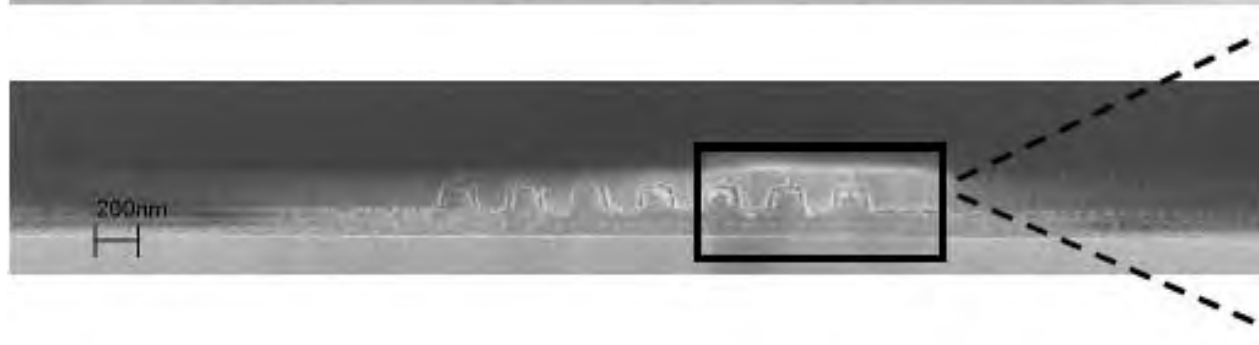
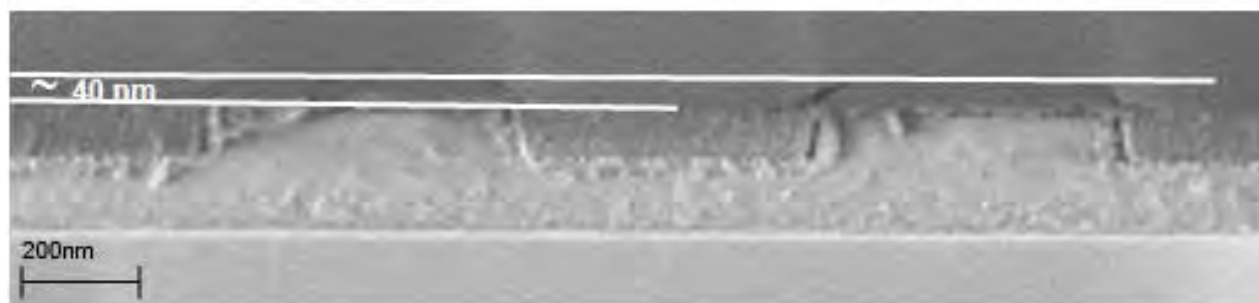
- to make HSQ harder

HSQ: hydrogen silsesquioxane

NIL of Interdigitated transducers: HSQ planarization



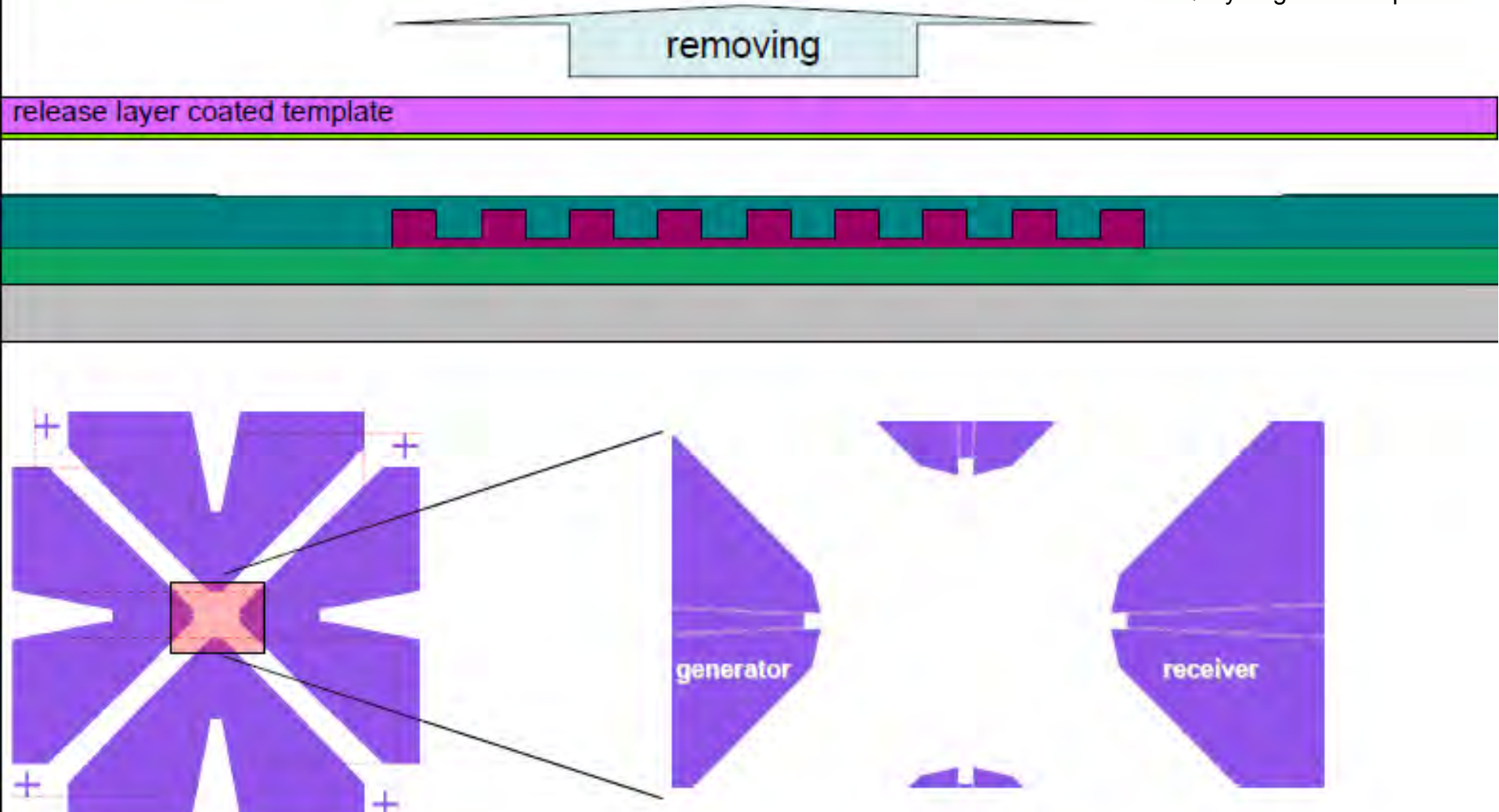
- Planarization quality decreases with feature size and spatial separation
- Appropriate planarization can not be achieved by applying simple “spin coating” method



S. Büyükköse, B. Vratzov and W GvdW, J. Vac. Sci. Technol. B **29**, 2 (2011).

NIL of Interdigitated transducers: HSQ planarization

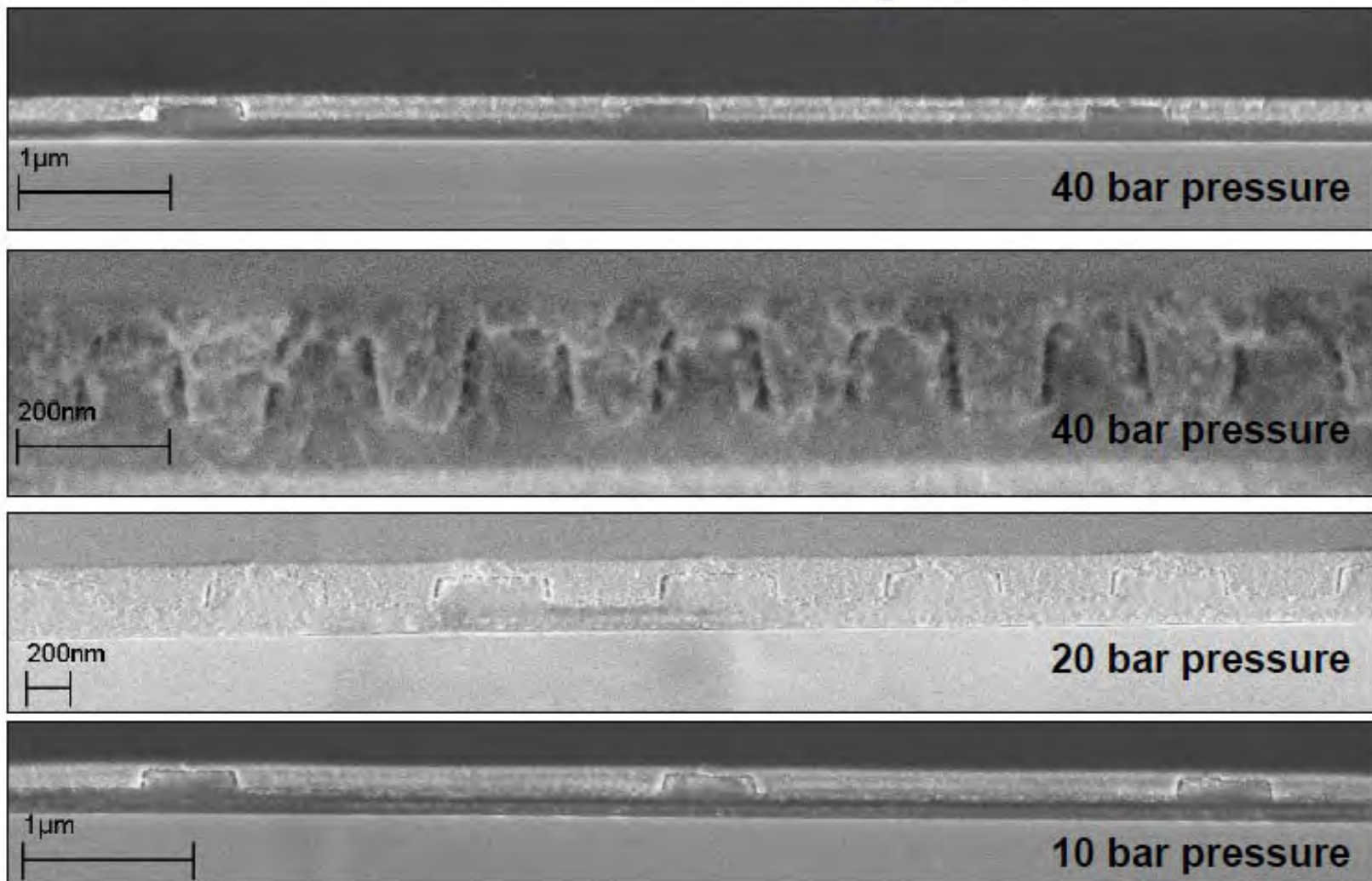
HSQ: hydrogen silsesquioxane



S. Büyükköse, B. Vratzov and W GvdW, J. Vac. Sci. Technol. B **29**, 2 (2011).

NIL of Interdigitated transducers: HSQ planarization

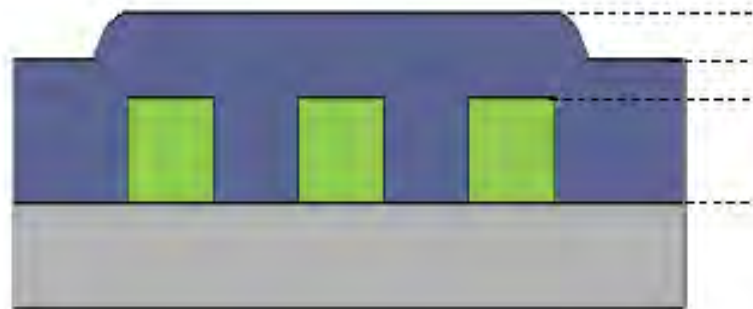
HSQ: hydrogen silsesquioxane



S. Büyükköse, B. Vratzov and W GvdW, J. Vac. Sci. Technol. B **29**, 2 (2011).

NIL of Interdigitated transducers: HSQ planarization

HSQ: hydrogen silsesquioxane



T_f (final step height)

T_i (initial step height)

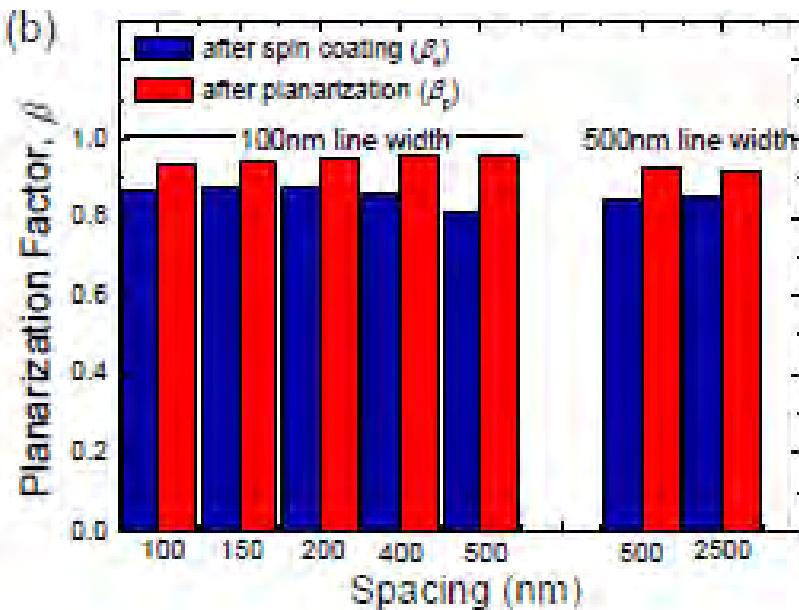
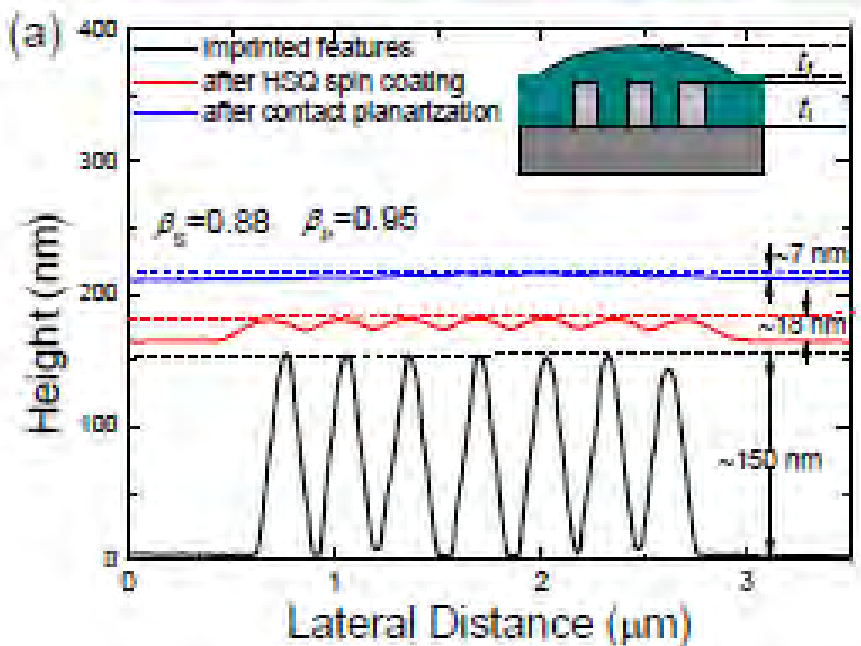
Planarization factor

$$\beta = (1 - T_f / T_i)$$

or

Degree of planarization

$$DOP(\%) = 100 \times \beta$$



NIL of Interdigitated transducers

5 Planarized sample



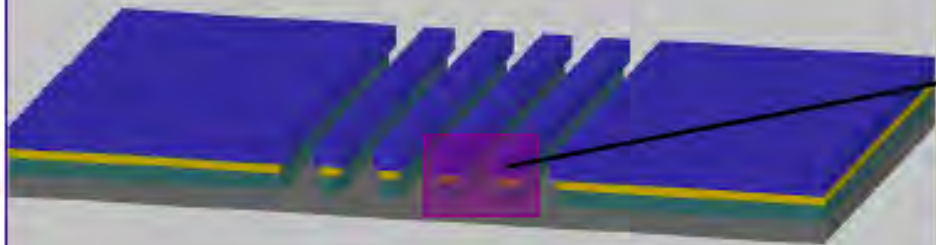
step height reduction about 95%

6 CHF₃ plasma based RIE



exposing elevated features

7 O₂ plasma based RIE

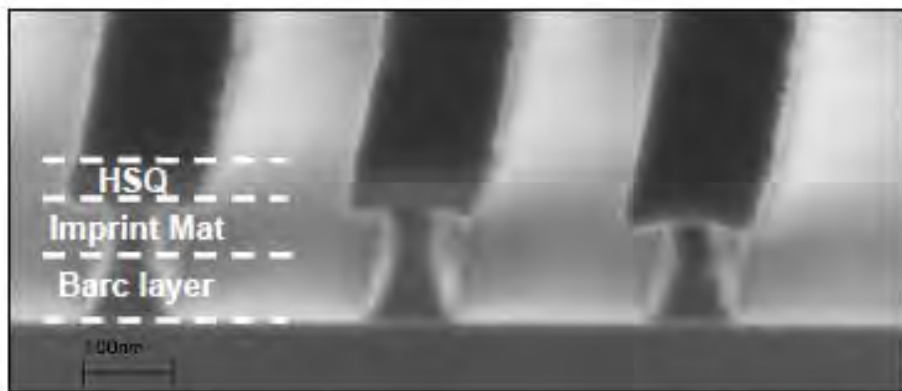
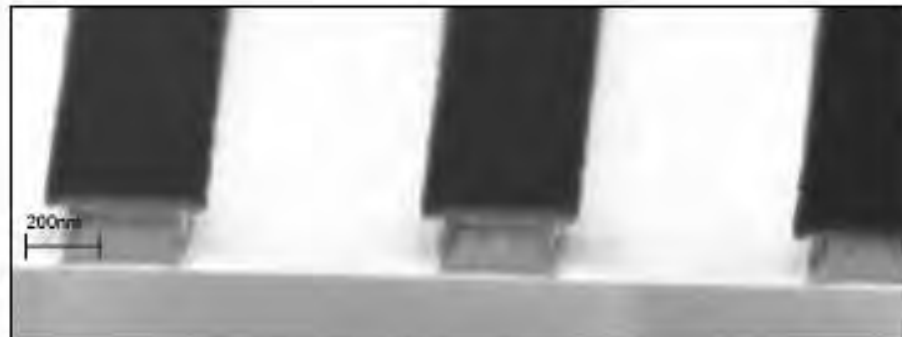
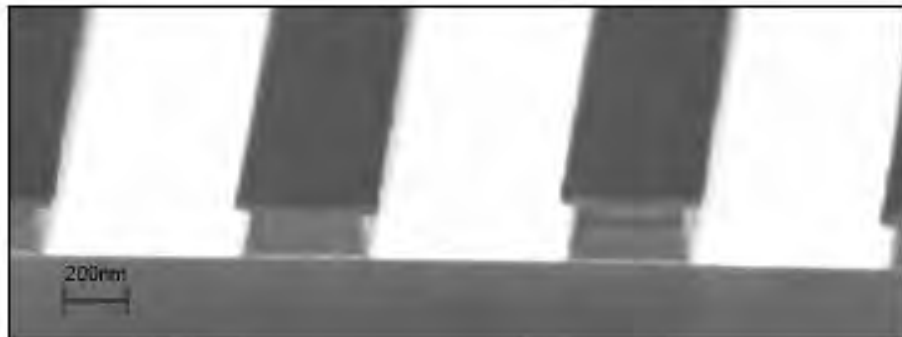


pattern transfer down to the substrate

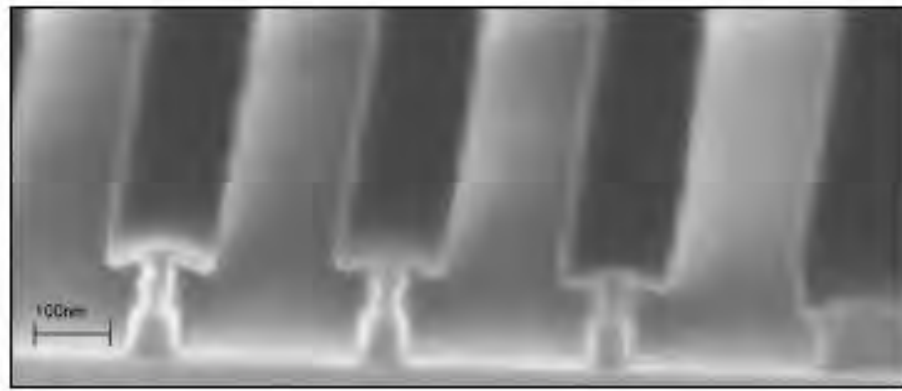


desired side-wall profile (under-cutting)

NIL of Interdigitated transducers



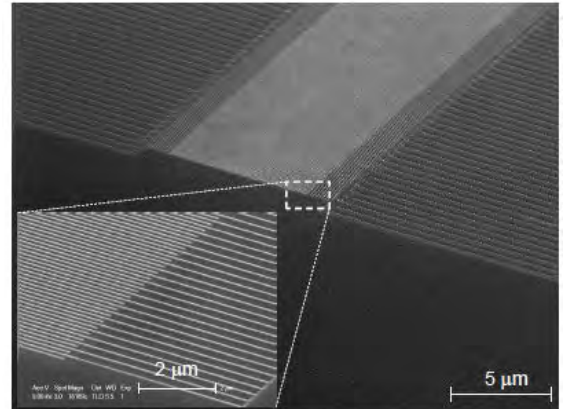
HSQ/Organic/Imp.Mat/Barc layer coated samples etched under CHF_3 plasma for **4.2 min.** and following O_2 plasma for **2 min.**



HSQ/Organic/Imp.Mat/Barc layer coated samples etched under CHF_3 plasma for **4.2 min.** and following O_2 plasma for **3 min.**

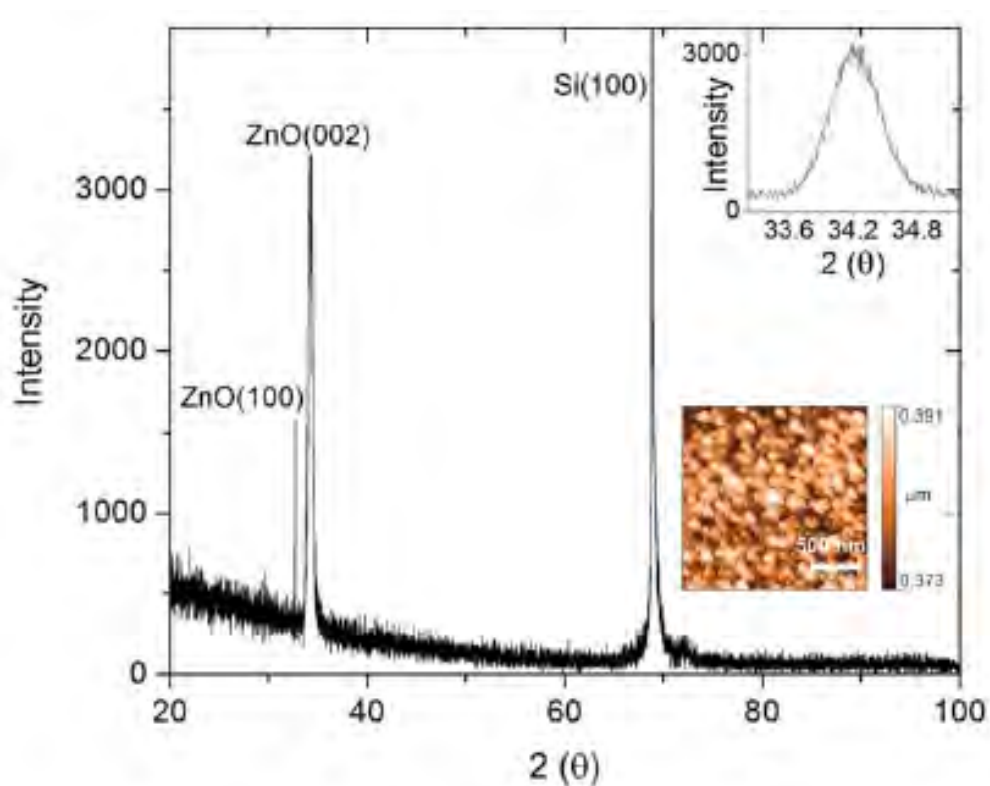
IDTs on a ZnO/SiO₂/Si multi-layer

- ZnO(230 nm)/SiO₂(100 nm)/Si multilayer
- SiO₂ buffer layer increases electromechanical coupling
- Sharply varying elastic properties → higher-order SAW modes
- ZnO: high electromechanical coupling constant, easy to fabricate (sputter)
- Double-sided polished (low-resistive) p-type (100) Si substrate (5-10 Ωcm)



S. Büyükköse, B. Vratzov, D. Atac, J. van der Veen, P. V. Santos and W GvdW,
Nanotechnology **23**, 315303 (2012).

IDTs on a ZnO/SiO₂/Si multi-layer



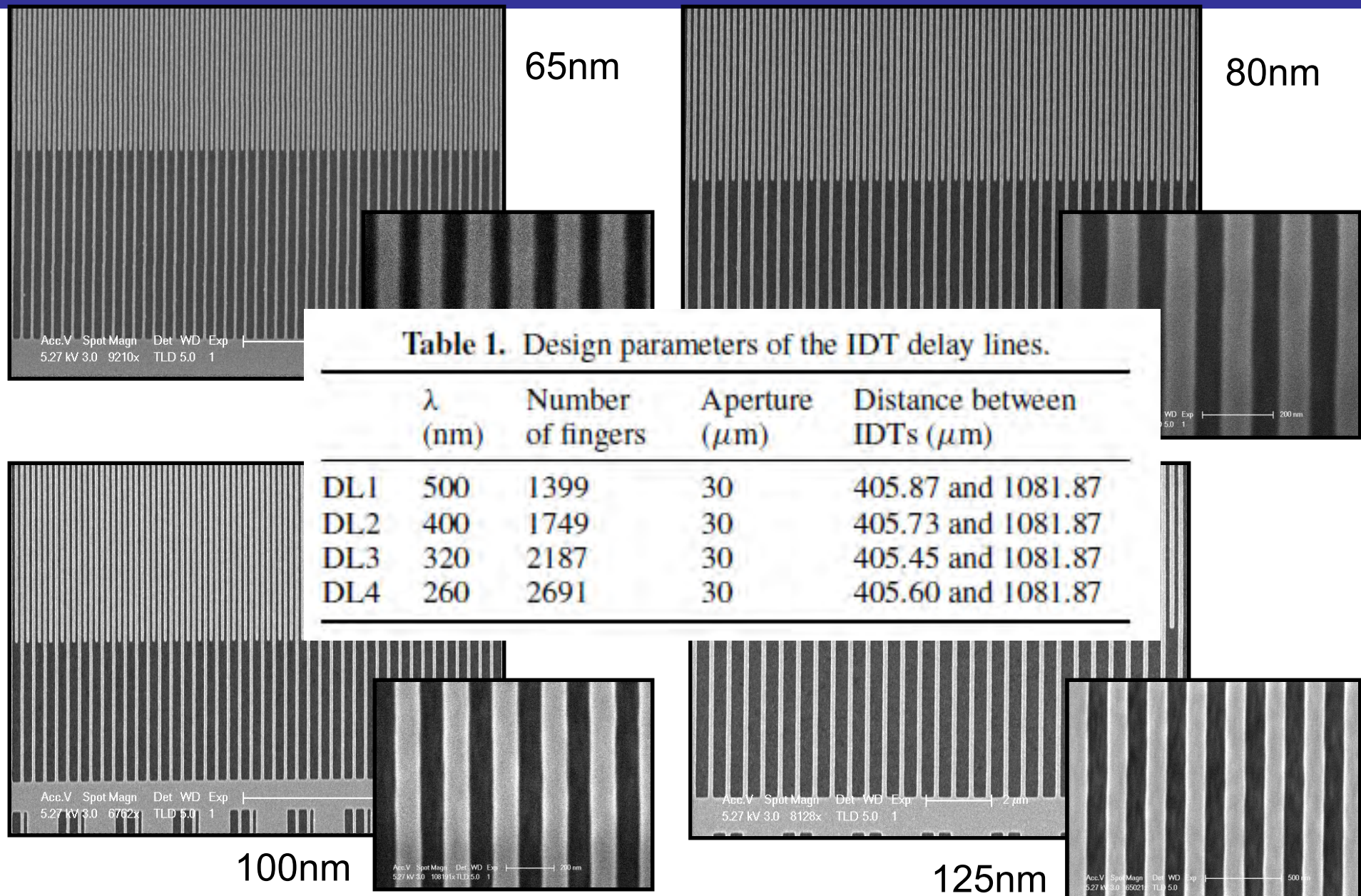
ZnO

- RF sputtering
- Wurtzite symmetry with hexagonal unit cell
- (002) surface has the smallest surface energy → c-axis (002) perpendicular to surface
- Highly c-axis oriented ZnO gives highest piezoelectricity
- Polycrystalline, ~15 nm grain size
- RMS ~ 2.5 nm

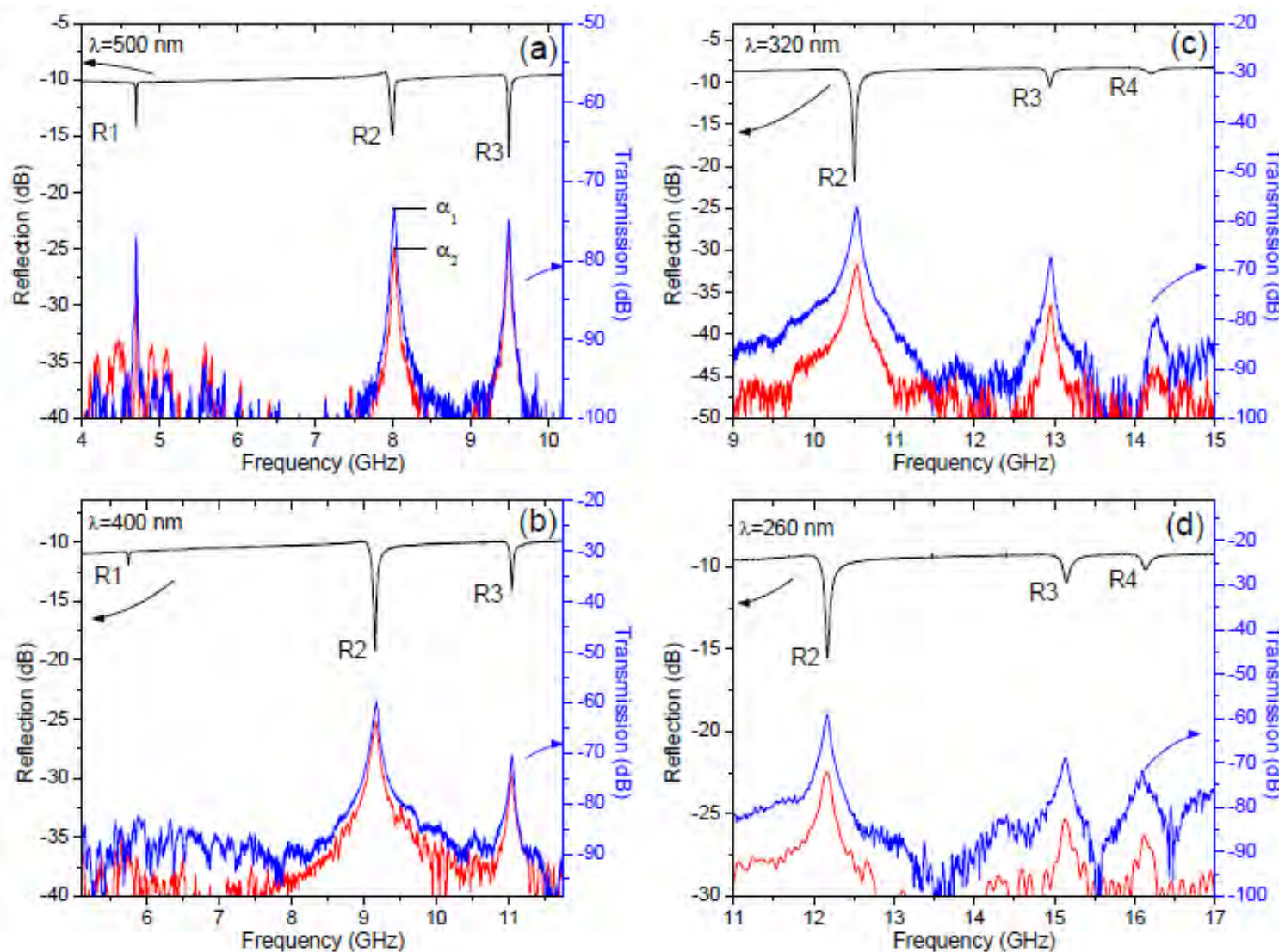
Collaboration with Dr. Yusuf Selamet Izmir Institute of Technology,
Turkey

S. Büyükköse, B. Vratzov, D. Atac, J. van der Veen, P. V. Santos and WGvdW,
Nanotechnology **23**, 315303 (2012).

IDTs on a ZnO/SiO₂/Si multi-layer



IDTs on a ZnO/SiO₂/Si multi-layer



R_n : nth Rayleigh mode

Blue: 405 um separation; Red: 1081 um separation

S. Büyükköse, B. Vratzov, D. Atac, J. van der Veen, P. V. Santos and W.GvdW, Nanotechnology **23**, 315303 (2012).

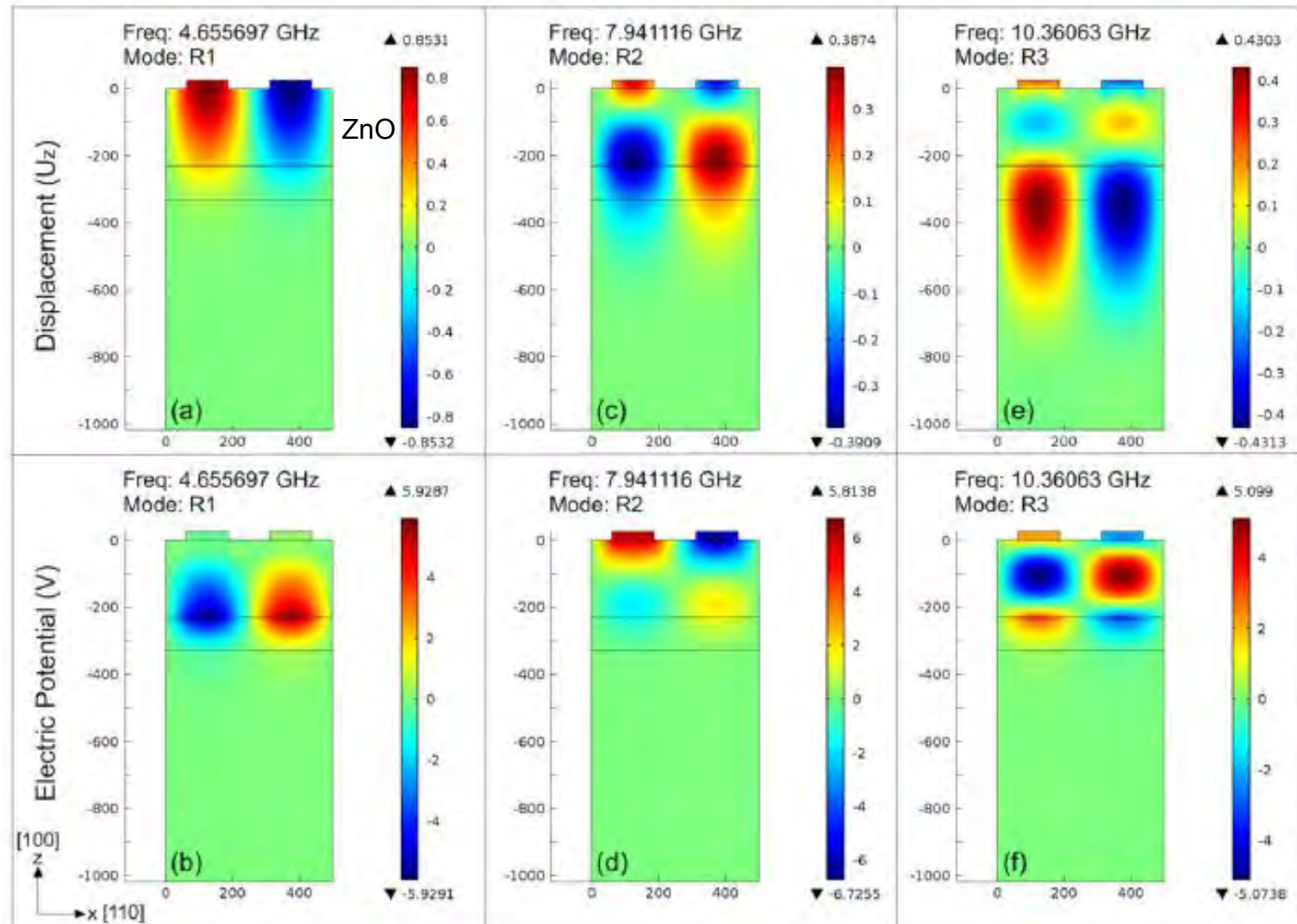
Higher-order Rayleigh modes

- Appear when the acoustic velocity in the overlayer(s) is lower than in the substrate
- $v_{\text{SAW},\text{Si}} > v_{\text{SAW},\text{SiO}_2}, v_{\text{SAW},\text{ZnO}}$
- Determined by the relative thickness of the film ($d_{\text{ZnO}} / \lambda_{\text{SAW}}$)

Table 2. Experimental results of resonance frequency, velocity and electromechanical coupling coefficient for different excitation modes of DL1 ($\lambda = 500$ nm), DL2 ($\lambda = 400$ nm), DL3 ($\lambda = 320$ nm) and DL4 ($\lambda = 260$ nm) devices. R1, R2, R3 and R4 are first-order (fundamental), second-order, third-order and fourth-order Rayleigh modes, respectively.

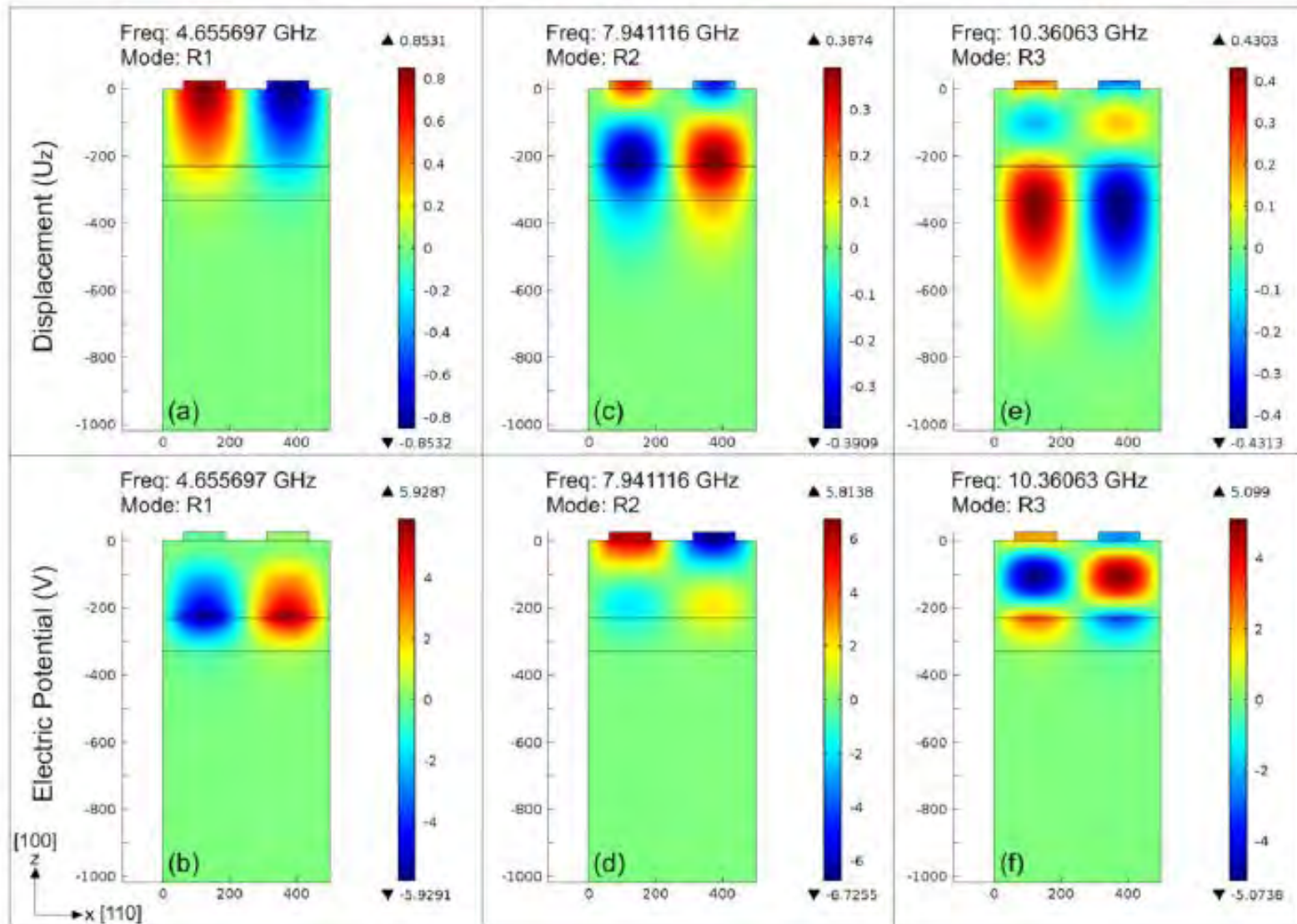
DL	R1			R2			R3			R4		
	f (GHz)	v (m s ⁻¹)	k^2	f (GHz)	v (m s ⁻¹)	k^2	f (GHz)	v (m s ⁻¹)	k^2	f (GHz)	v (m s ⁻¹)	k^2
1	4.697	2348	0.007	8.002	4001	0.030	9.495	4747	0.010	—	—	—
2	5.737	2295	0.012	9.137	3655	0.036	11.03	4412	0.014	—	—	—
3	—	—	—	10.54	3373	0.032	12.96	4147	0.013	14.26	4563	0.025
4	—	—	—	12.17	3164	0.033	15.14	3937	0.031	16.13	4194	0.028

Higher-order Rayleigh modes (simulations), $\lambda = 500$ nm



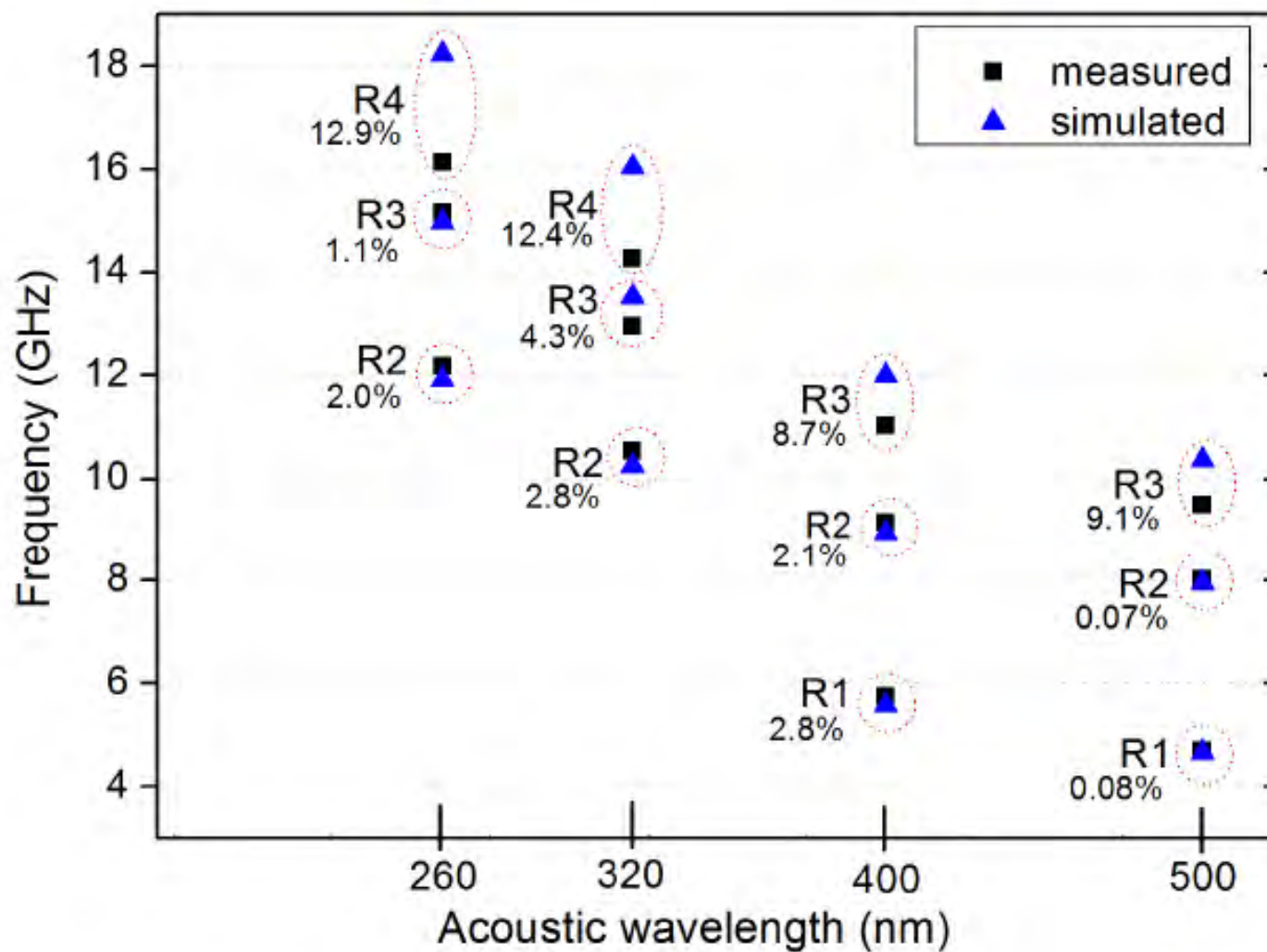
S. Büyükköse, B. Vratzov, D. Atac, J. van der Veen, P. V. Santos and W.GvdW, Nanotechnology **23**, 315303 (2012).

Higher-order Rayleigh modes (simulations), $\lambda = 260$ nm



S. Büyükköse, B. Vratzov, D. Atac, J. van der Veen, P. V. Santos and W.GvdW, Nanotechnology **23**, 315303 (2012).

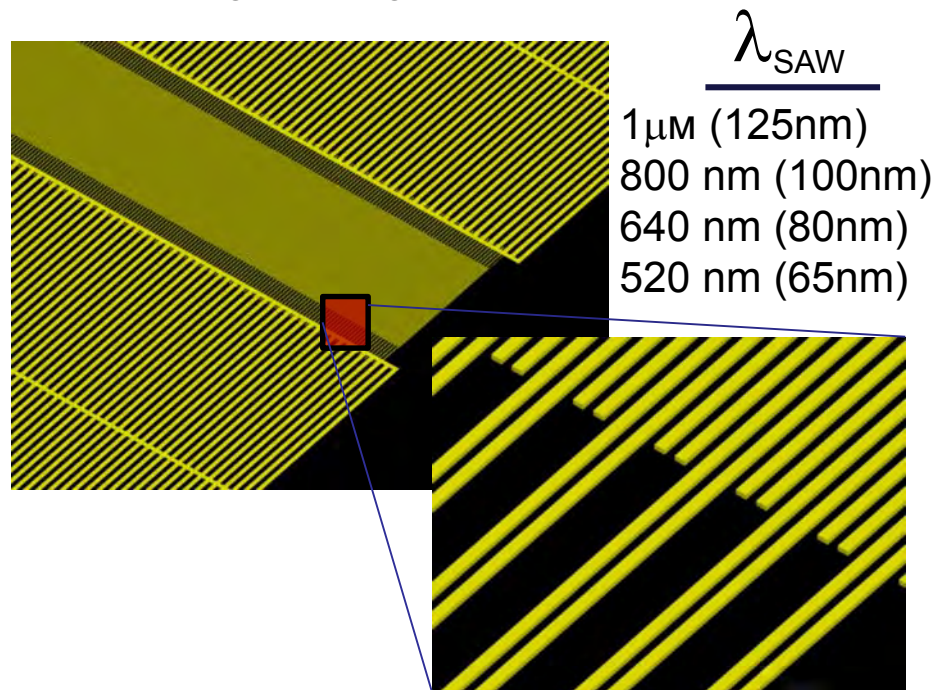
Higher-order Rayleigh modes: comparison



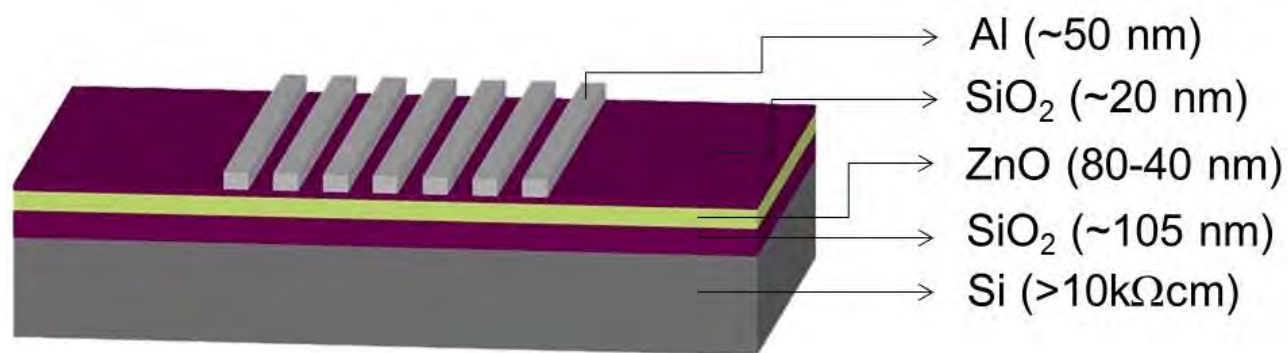
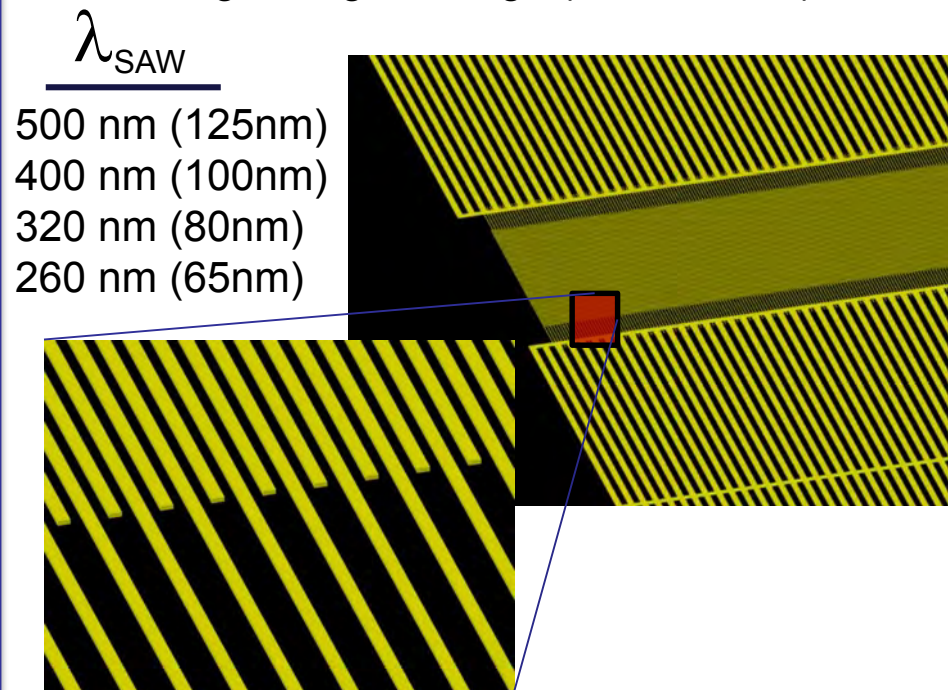
S. Büyükköse, B. Vratzov, D. Atac, J. van der Veen, P. V. Santos and W.GvdW, Nanotechnology **23**, 315303 (2012).

IDTs on a $\text{SiO}_2/\text{ZnO}/\text{SiO}_2/\text{Si}$ multi-layer

Double Finger Design ($\text{ZnO}=80 \text{ nm}$)

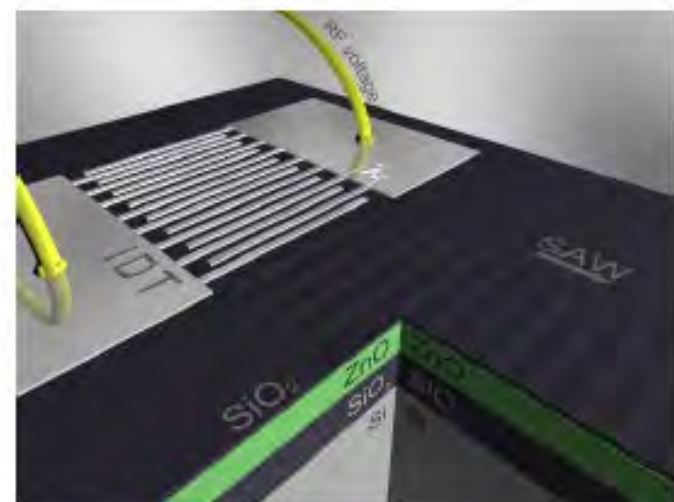
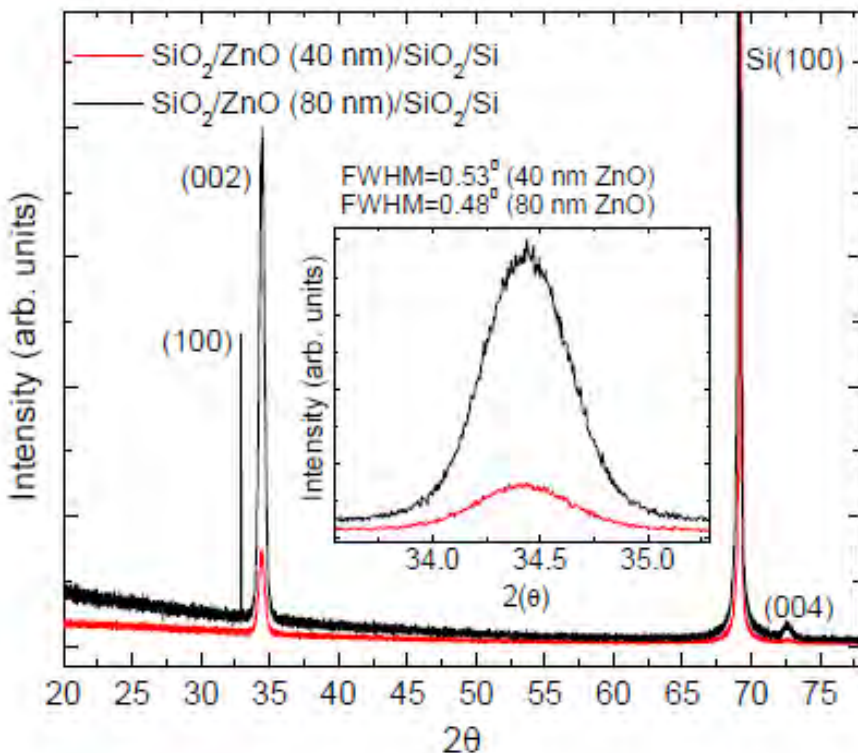


Single Finger Design ($\text{ZnO}=40 \text{ nm}$)



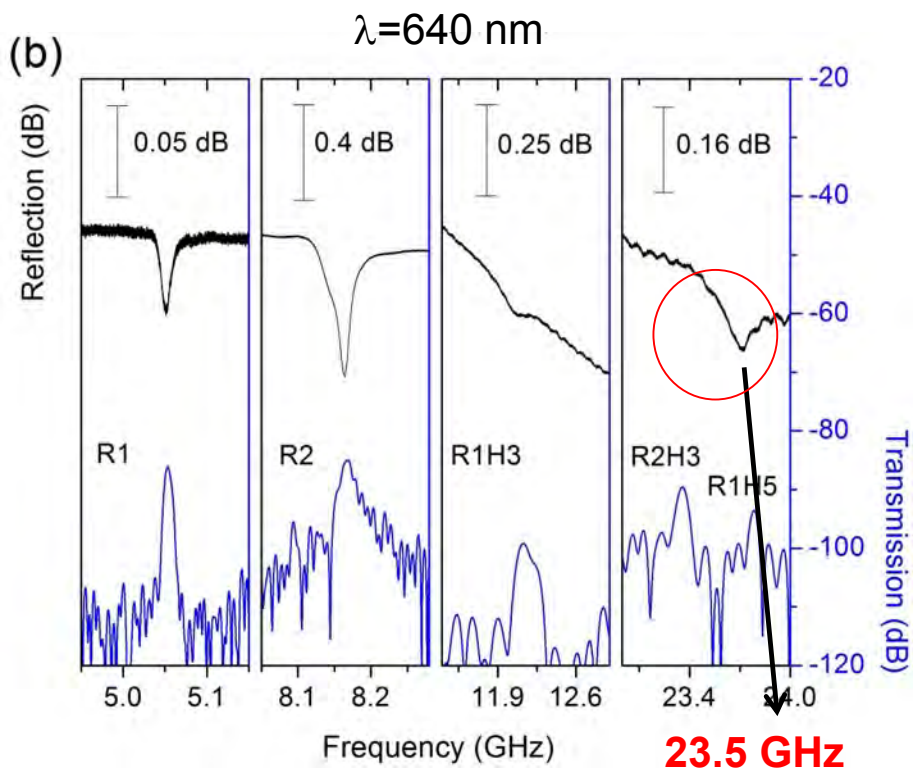
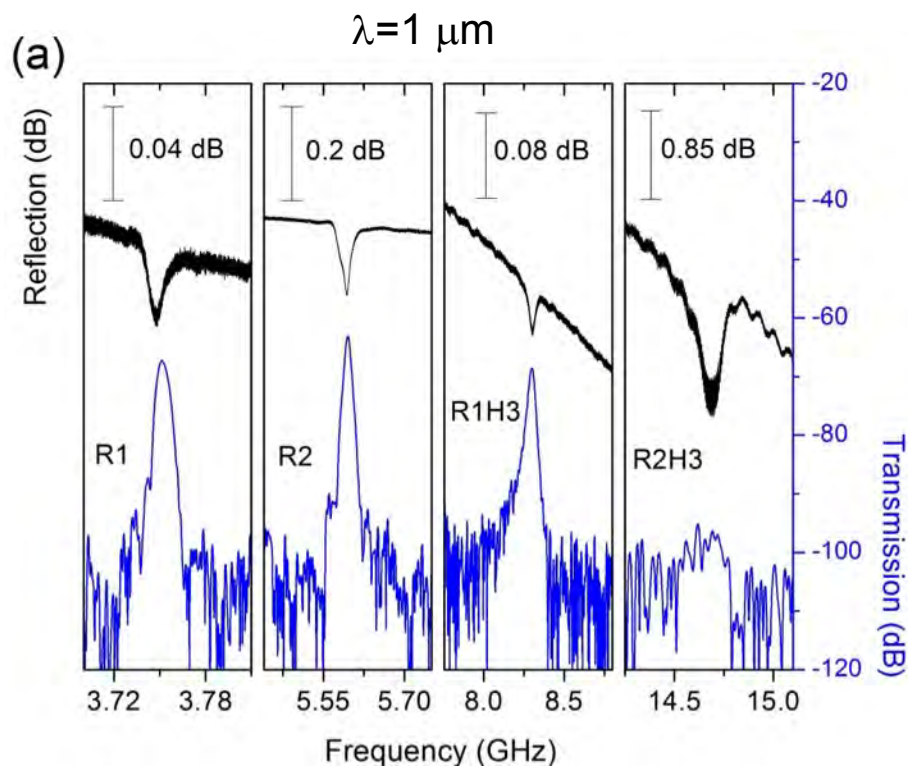
IDTs on a $\text{SiO}_2/\text{ZnO}/\text{SiO}_2/\text{Si}$ multi-layer

- $\text{SiO}_2(20 \text{ nm})/\text{ZnO}(40,80 \text{ nm})/\text{SiO}_2(105 \text{ nm})/\text{Si}$ multilayer
- Unprotected ZnO is CMOS incompatible
- Substrate is a highly resistive Si ($>10 \text{ k}\Omega$) wafer



S. Büyükköse, B. Vratzov, J. van der Veen, P. V. Santos and WGvdW
Appl. Phys. Lett. 102, 013112 (2013).

SAW Characterisation



R_n – nth Rayleigh mode

RnH3 – 3rd Harmonics

S. Büyükköse, B. Vratzov, J. van der Veen, P. V. Santos and W GvdW
Appl. Phys. Lett. **102**, 013112 (2013).

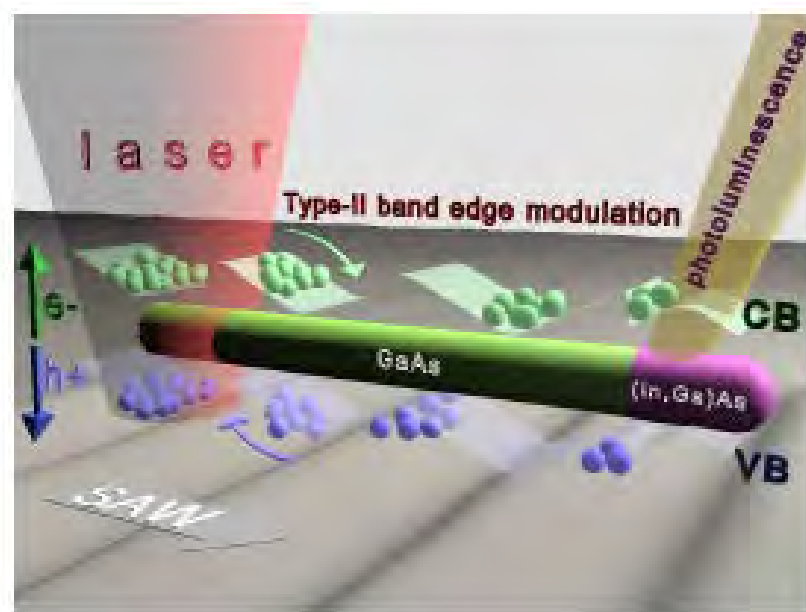
High-frequency acoustic charge transport in GaAs nanowires

- Semiconductor nanowires (NWs) offer new possibilities for low-dimensional optoelectronic devices.
- The operation of such devices requires appropriate techniques for applying electrical control fields, which typically involve doping and contacting of nm-sized structures.
- An efficient carrier transport mechanism which eliminates electrical contact issue on nanostructures is important.

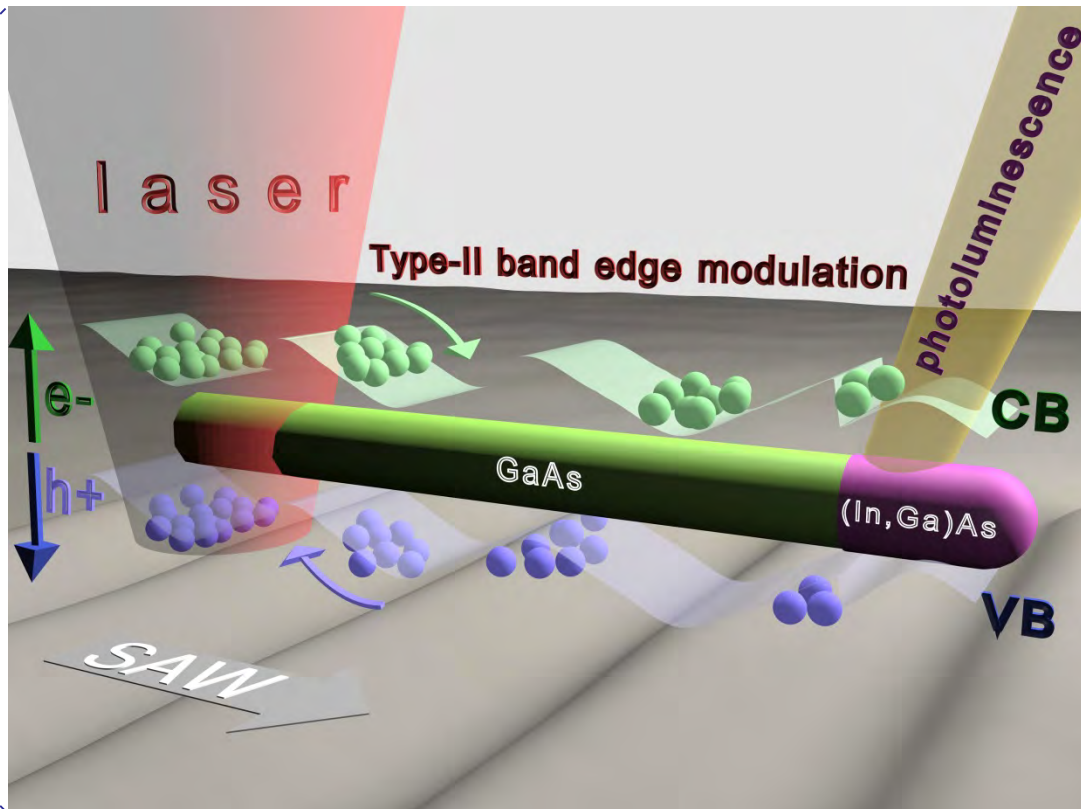
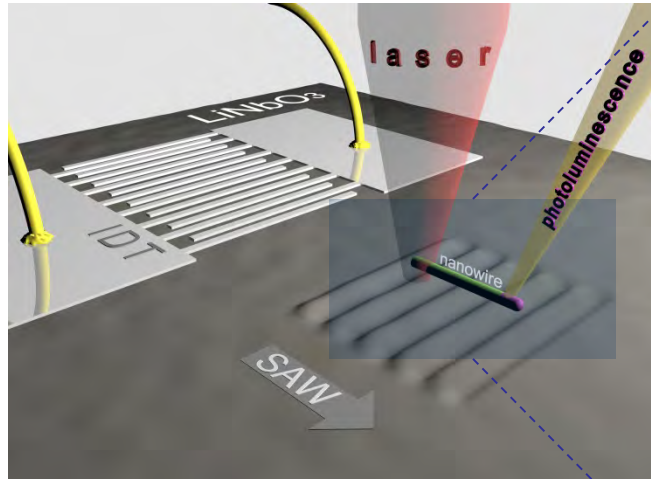
SAW enables contactless manipulation of carriers in semiconductors!



S Büyükköse, A Hernández-Mínguez, B Vratzov, C Somaschini, L Geelhaar, H Riechert, WGvdW and P V Santos, Nanotechnology **25**, 135204 (2014).



Experimental details: Measurement setup I

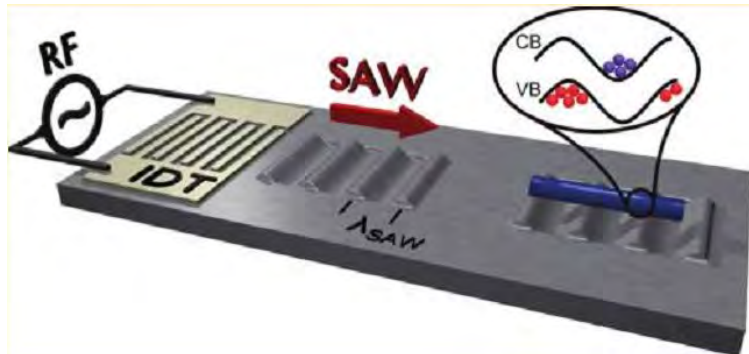


Ambipolar transport in NWs

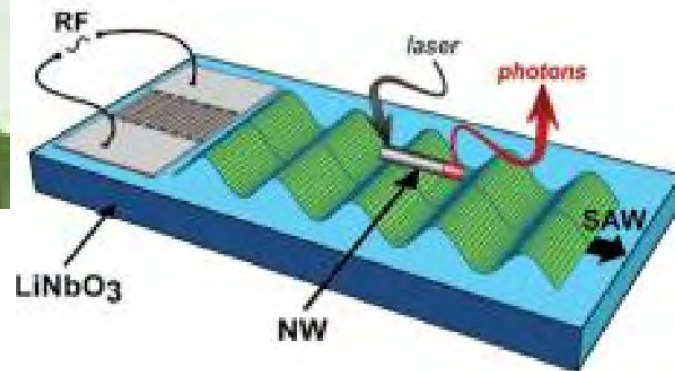
- SAW Induced type-II modulation of the band edges: $\lambda_{\text{SAW}} < L_{\text{NW}}$
- Excitation of electron-hole pairs by an incident laser pulse
- Spatial separation of e-h pairs due to the modulated conduction (CB) and valence band (VB)
- This prevents the recombination of the carriers and allows to transport the carriers at v_{SAW} .

Previous works on SAW induced ambipolar CT in NWs

J. B. Kinzel et al. Nano Lett. 2011, 11, 1512



A. Hernández-Míguez et al. Nano Lett. 2012, 12, 252



SAW controlled modulation of the optical emission of single GaAs NWs.
(no transport !)

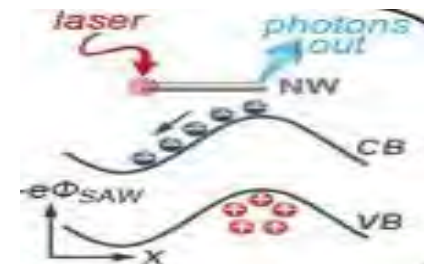
$$\lambda_{\text{SAW}} = 17.5 \mu\text{m} \text{ and } 5.5 \mu\text{m}$$

Length of NW= 15 μm

SAW induced ambipolar transport in GaAs/AlGaAs core/shell NWs.
(max. transport efficiency $\cong 50 \%$)

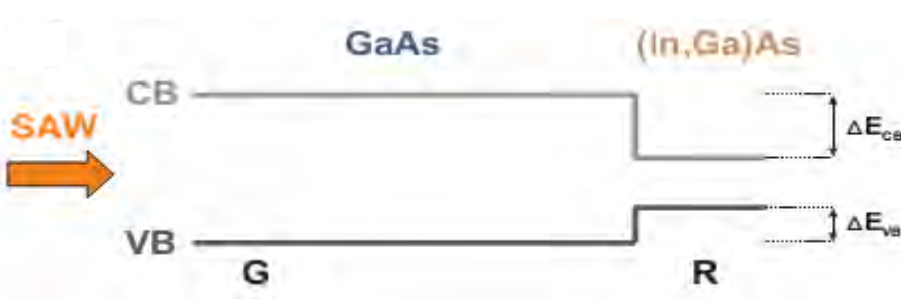
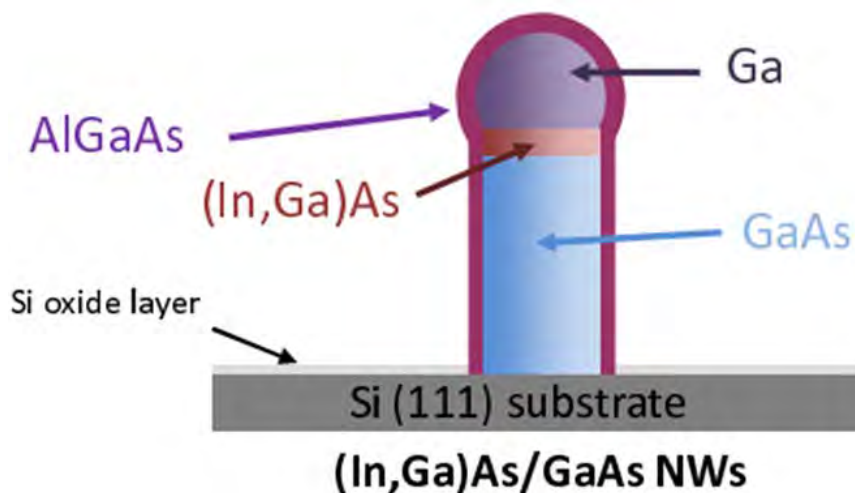
$$\lambda_{\text{SAW}} = 17.5 \mu\text{m}$$

Length of NW= 8 μm



$$\Phi_{\text{SAW}}(x, t) = \Phi_{\text{SAW}_0} \sin[2\pi(x/\lambda_{\text{SAW}}) - (t/T_{\text{SAW}})] , (x < \lambda_{\text{SAW}}^{34})$$

Experimental details: NW growth



Simple demonstration of band structure along growth direction

Breuer *et al.*, Nano Lett. **11**, 1276 (2011).

The GaAs NWs were grown by MBE using a self-assisted VLS method

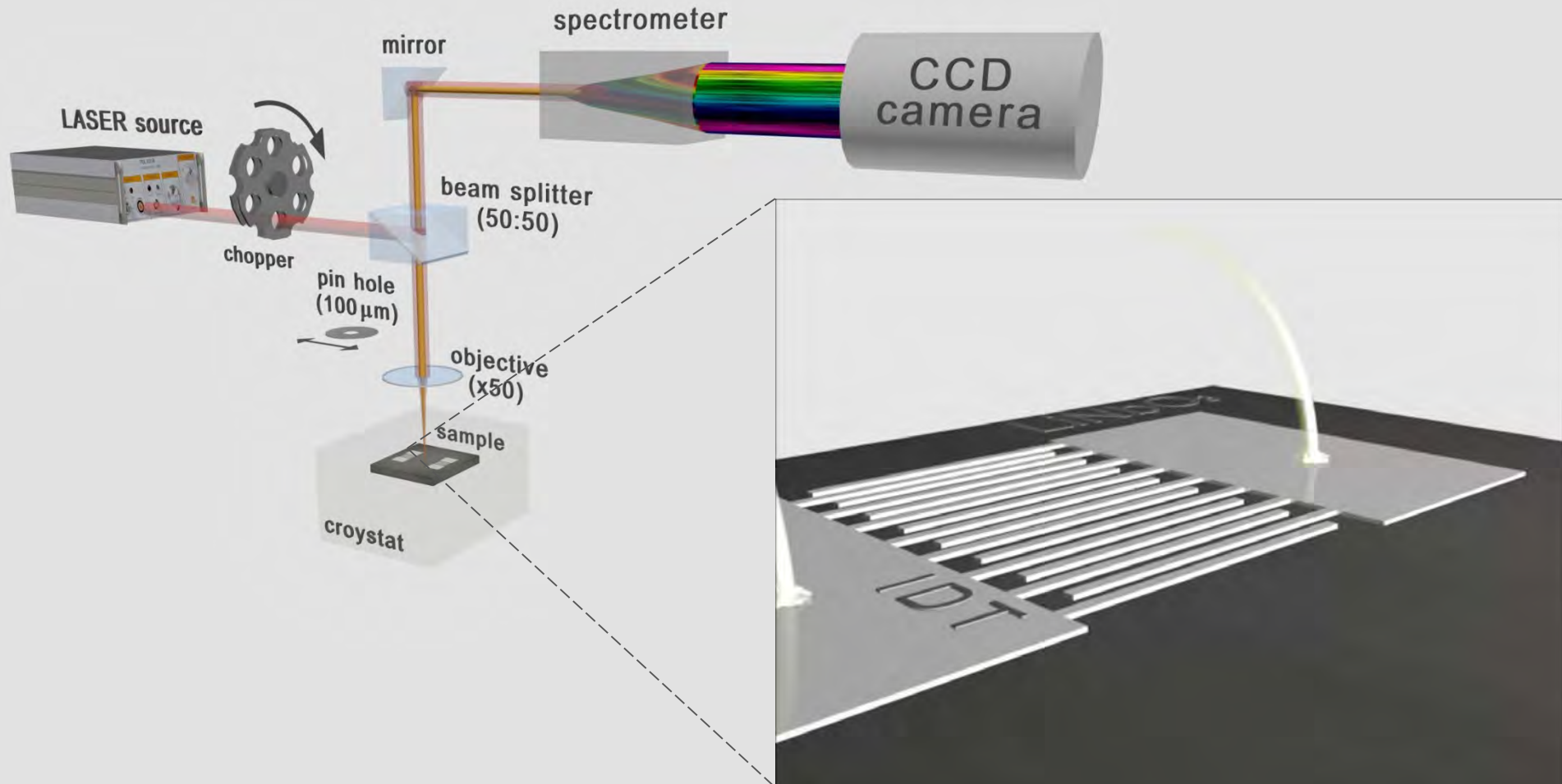
A segment of approx. 300 nm length containing In inclusions at the top of the GaAs section.

$Al_x Ga_{1-x} As$ shell ($x= 0.3$) was incorporated to prevent non-radiative recombination at the free surfaces.

Average length of 7 μm and diameter of 150 nm.

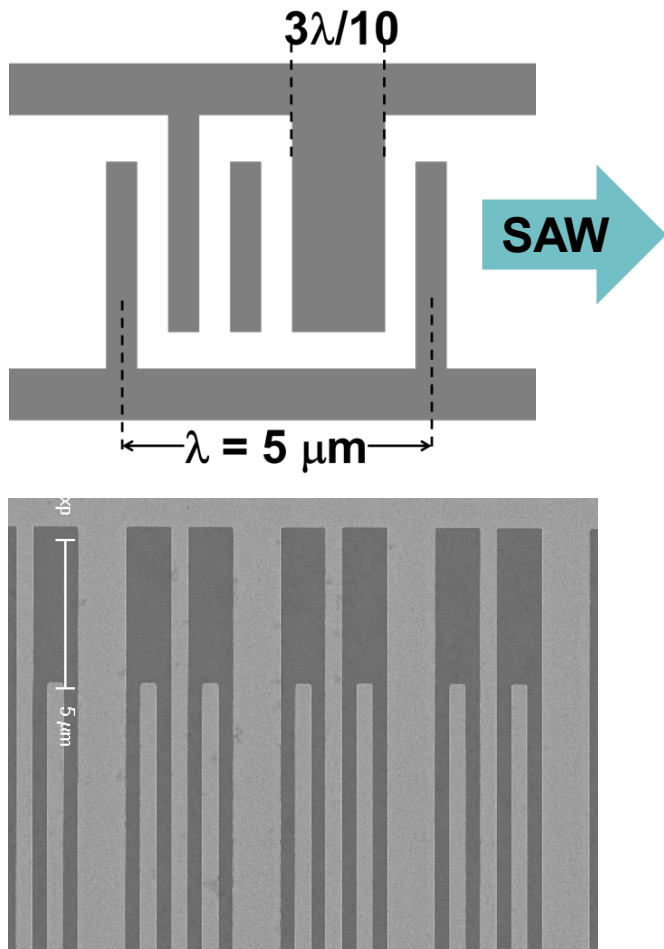
NWs were removed from the substrate and mechanically dispersed on a 128° Y-cut $LiNbO_3$ substrate

Experimental details: Measurement setup II

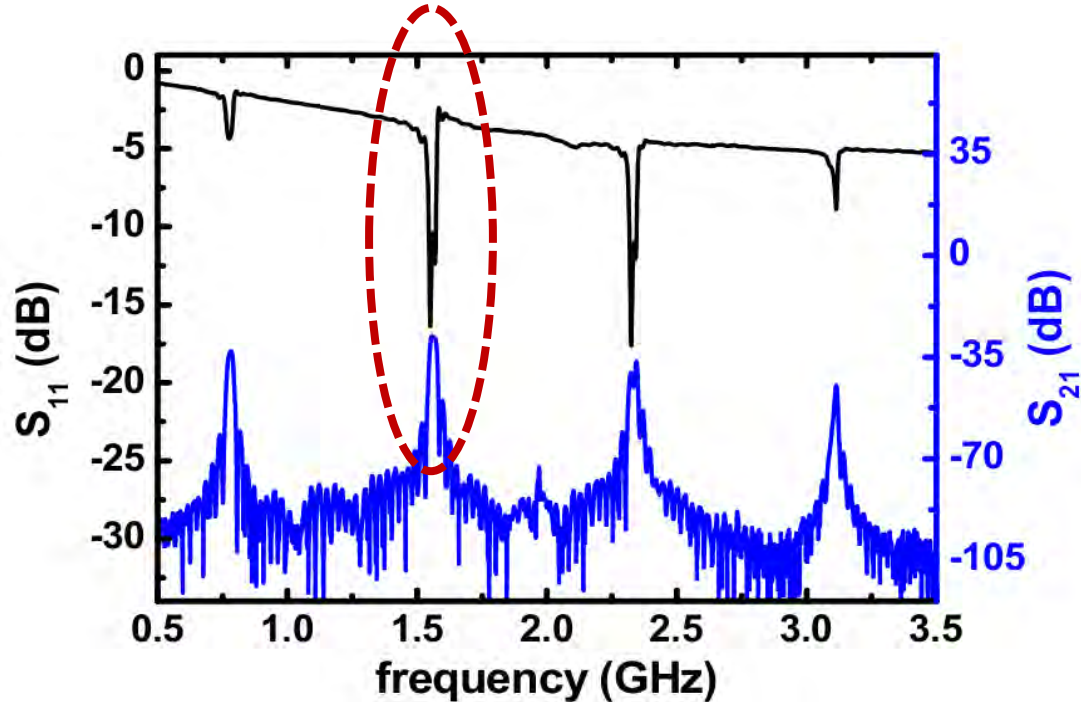


- Experiments performed at 20 K.
- A tightly focused (50X objective, spot diameter of $1.5\text{ }\mu\text{m}$) laser beam of wavelength 756 nm.
- PL is collected by the same objective that focuses the laser beam and sent to the input of a spectrometer connected to a charge-coupled device (CCD) camera.

Results: Frequency response of IDT



$\sim 1.57 \text{ GHz}$



$$\lambda_{\text{SAW}} = 2.57 \text{ um} < L_{\text{NW}} \sim 7 \text{ um}$$

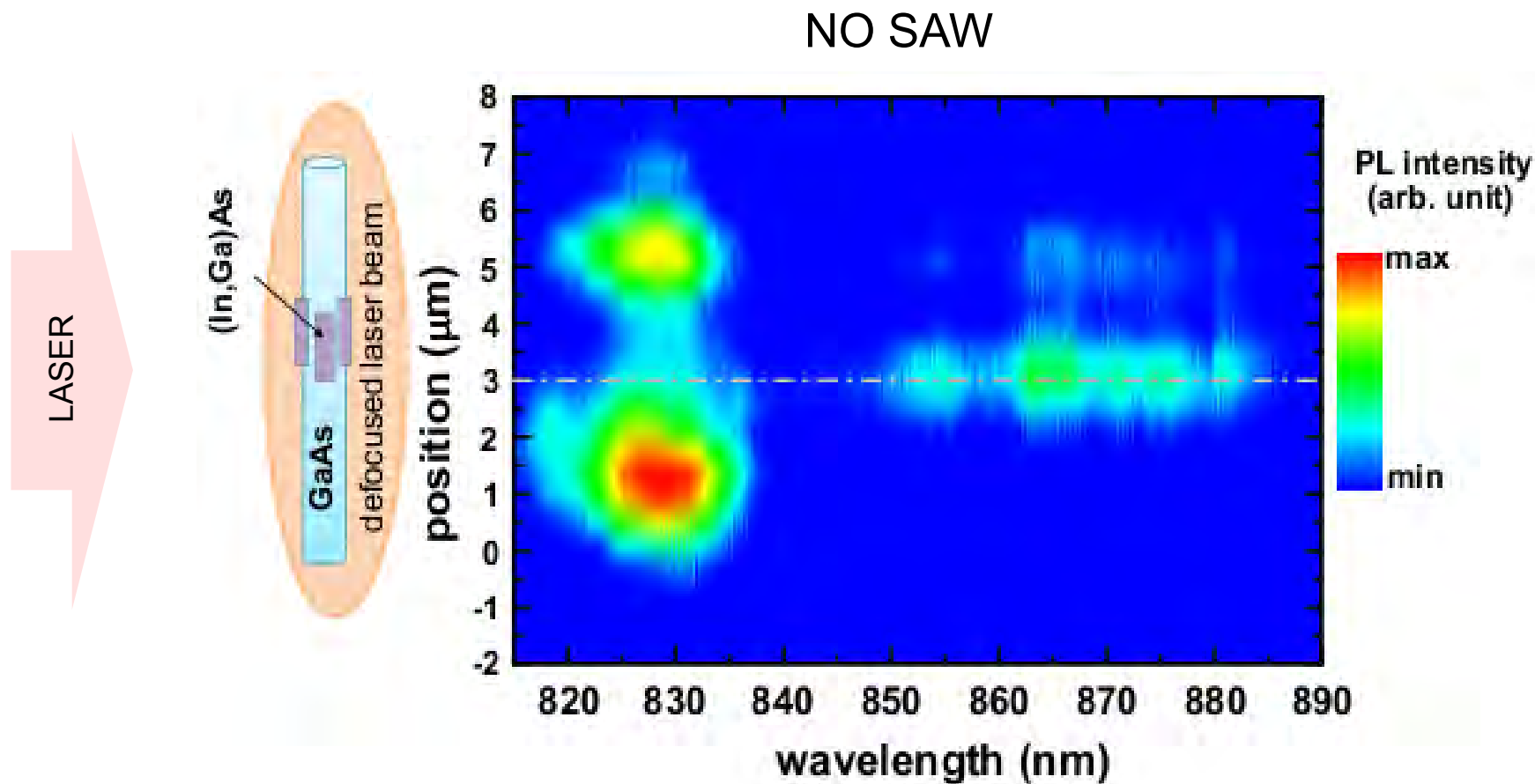
→ Simultaneous transport of electrons and holes in the **SAME** direction

Floating-electrode unidirectional transducer (FEUDT) → higher SAW amplitudes

S Büyükköse, A Hernández-Mínguez, B Vratzov, C Somaschini, L Geelhaar, H Riechert, W GvdW and P V Santos, Nanotechnology **25**, 135204 (2014).

Results: PL from NW under overall illumination

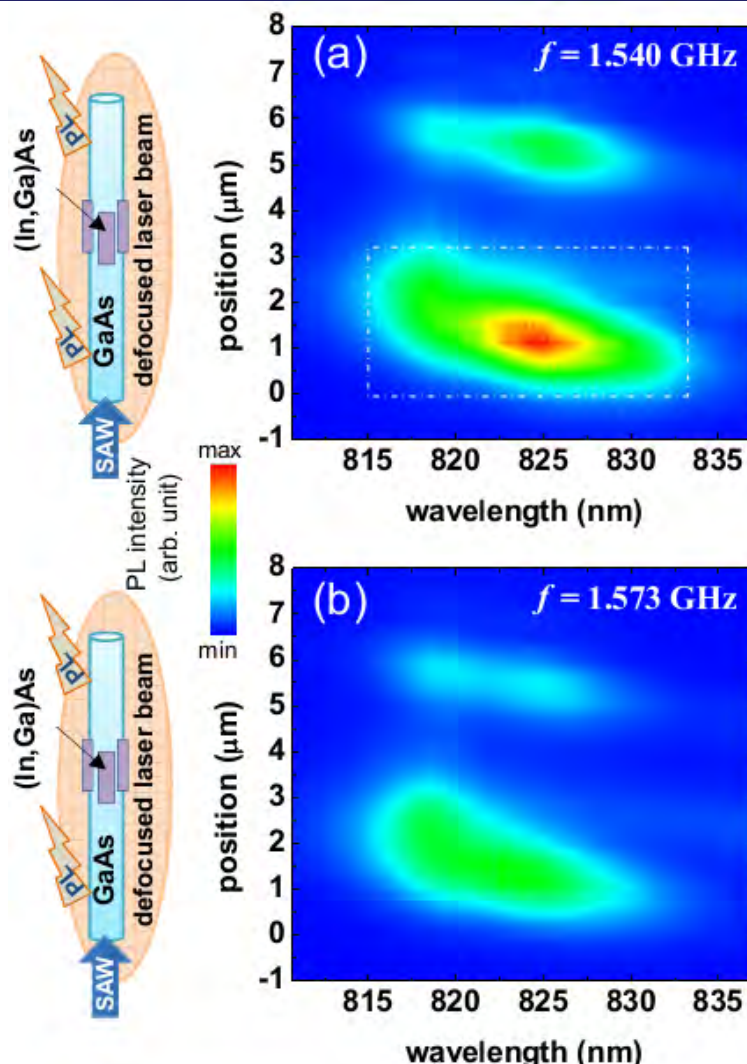
NW_1



S Büyükköse, A Hernández-Mínguez, B Vratzov, C Somaschini, L Geelhaar, H Riechert, W GvdW and P V Santos,
Nanotechnology **25**, 135204 (2014).

Results: PL emission from GaAs segment

NW_1

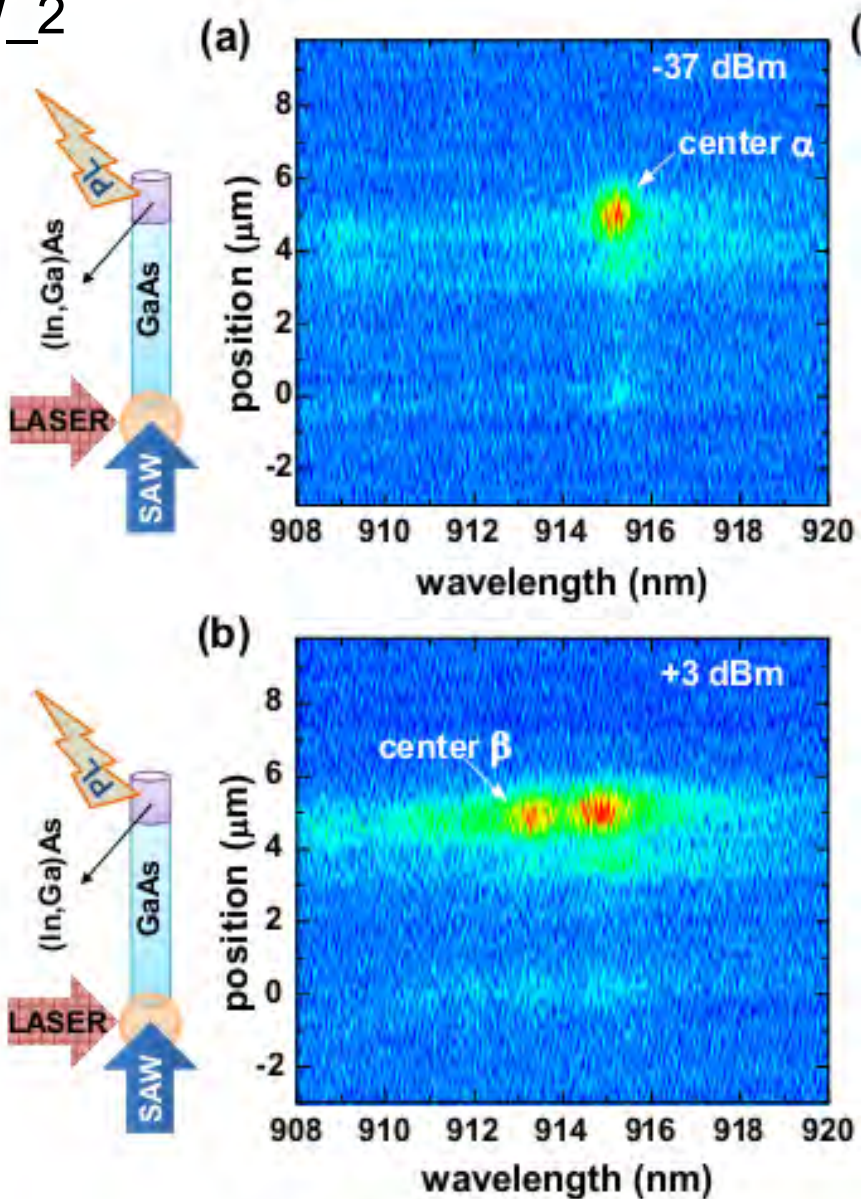


SAW off-resonance

SAW on-resonance
(40% suppression of PL)

Results: PL emission from (In,Ga)As segment

NW_2

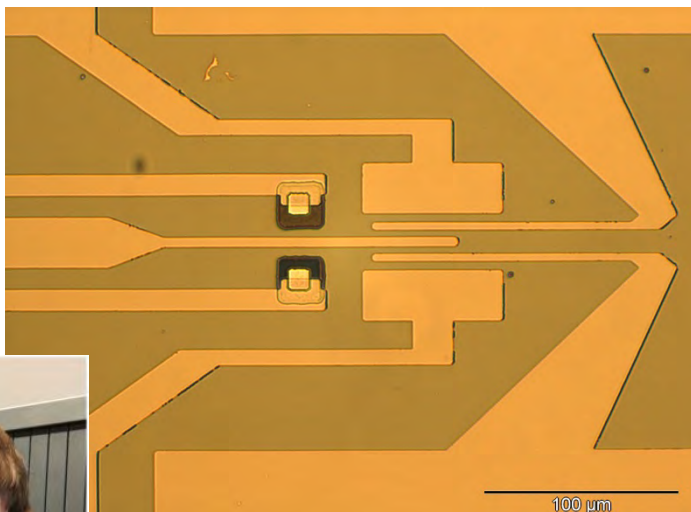


PL images of two recombination centres
at $x_r = 5 \mu\text{m}$ for two RF powers

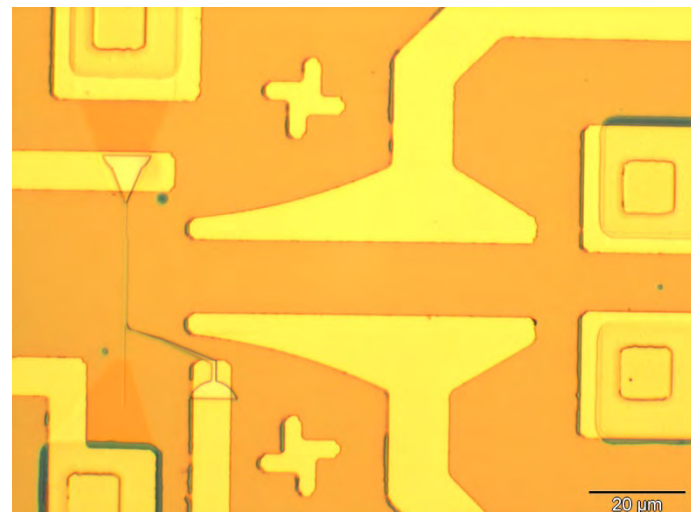
(a) $P_{RF} = -37 \text{ dBm}$, and (b) $P_{RF} = +3 \text{ dBm}$.

Future Work: Measurements on Si-SAW devices

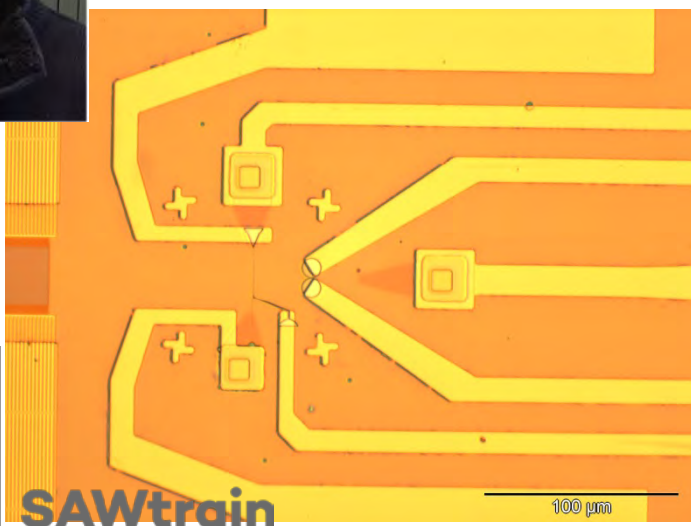
Photon detector



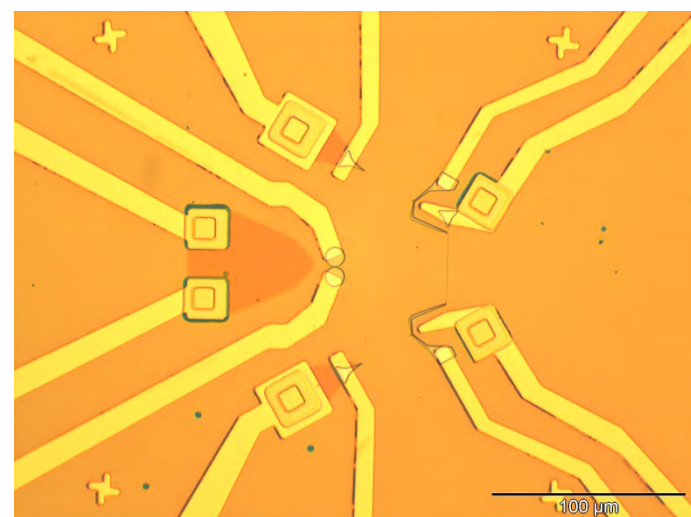
Acoustic switch



Single charge pumping

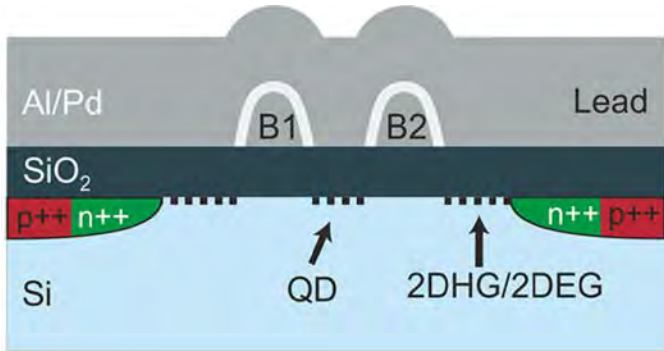


Single charge pumping (interfering SAW)

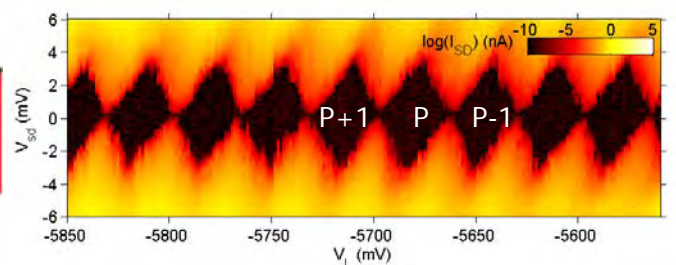
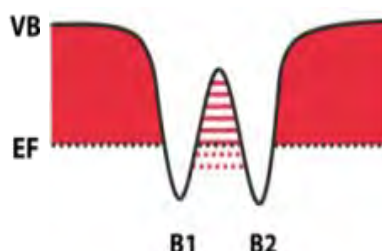
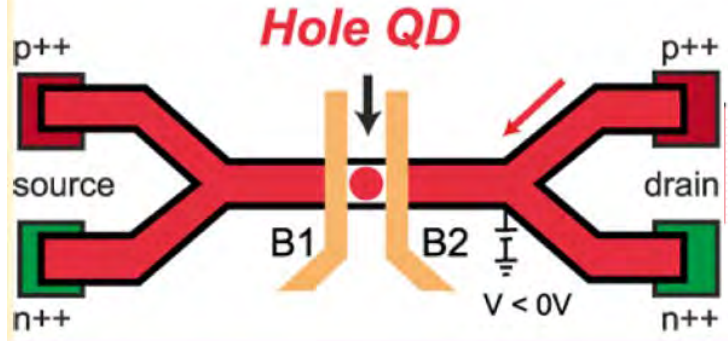
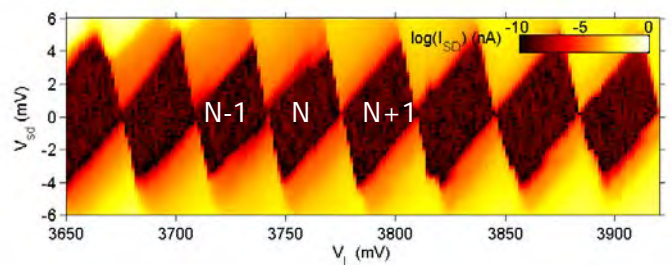
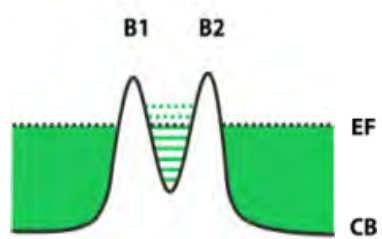
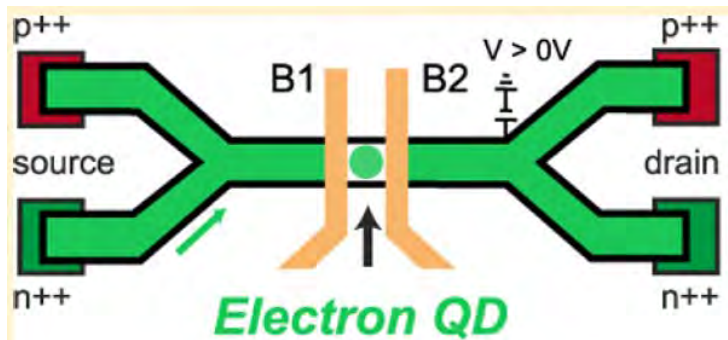
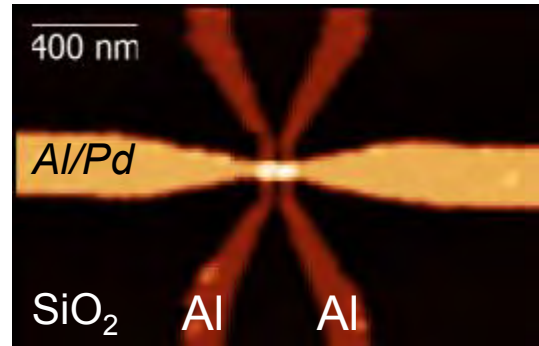


SAWtrain
network

AMBIOPOLAR QUANTUM DOTS IN NANOMOSFETS

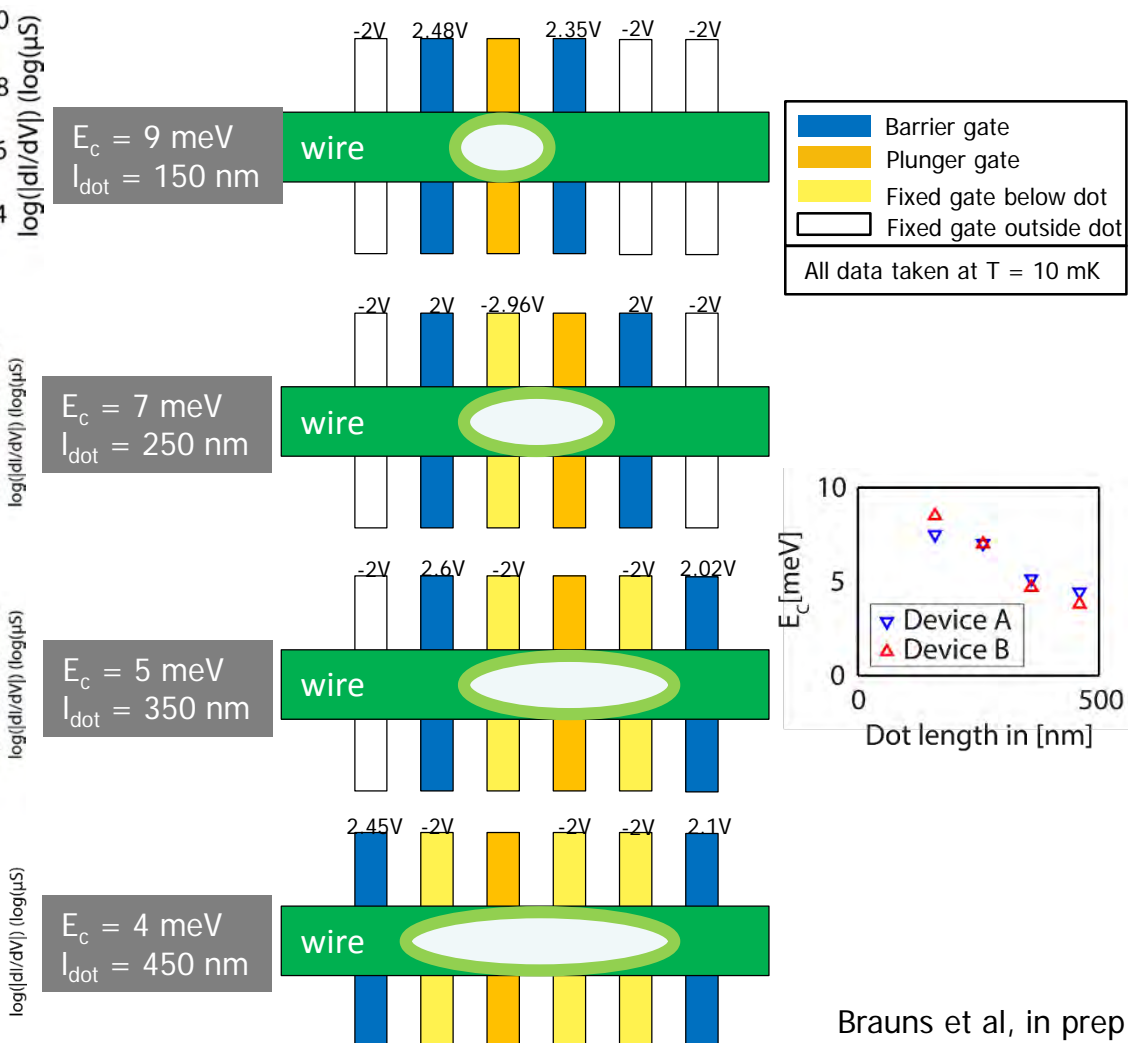
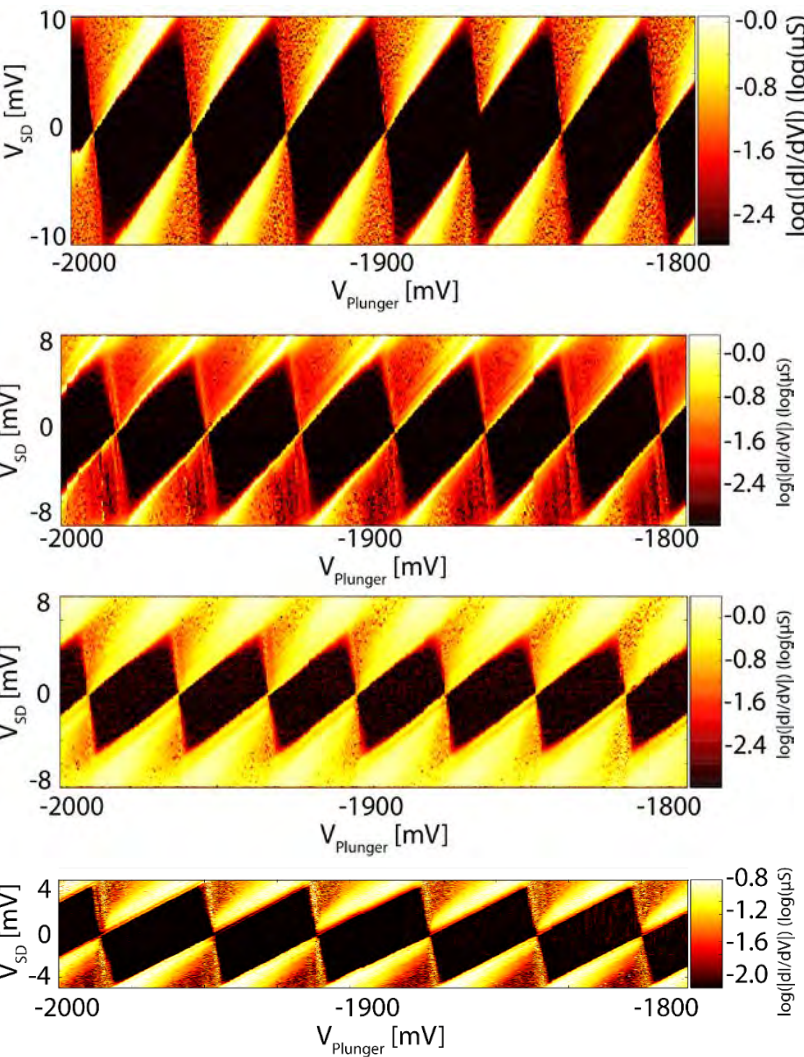


Compare single-hole tunneling with single-electron tunneling in one and the same device, i.e. with the same silicon, oxide, metal *and* impurities



Müller et al, Nano Lett 2015, APL 2015

GE/SI CORE/SHELL NANOWIRES

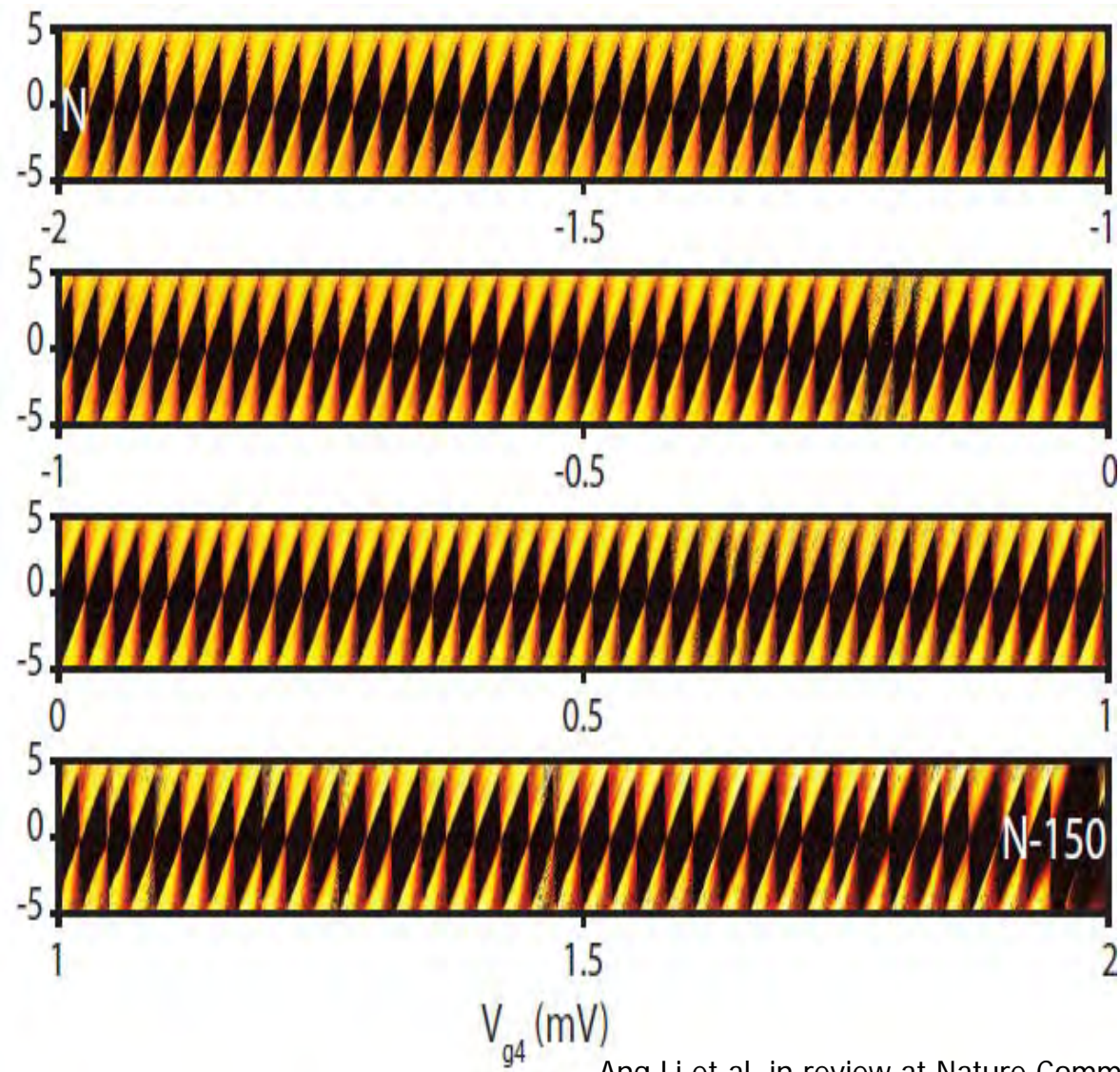
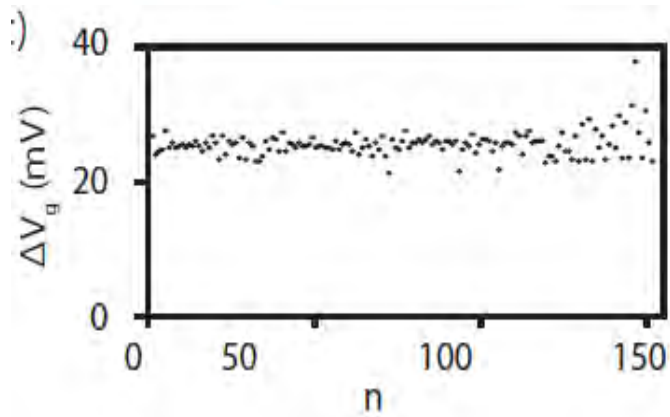
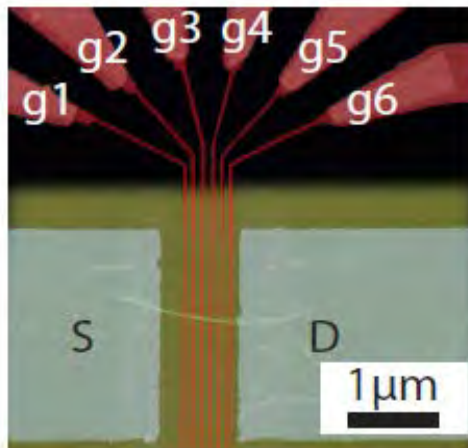


Brauns et al, in prep

Brauns et al, PRB Rap Comm 2016

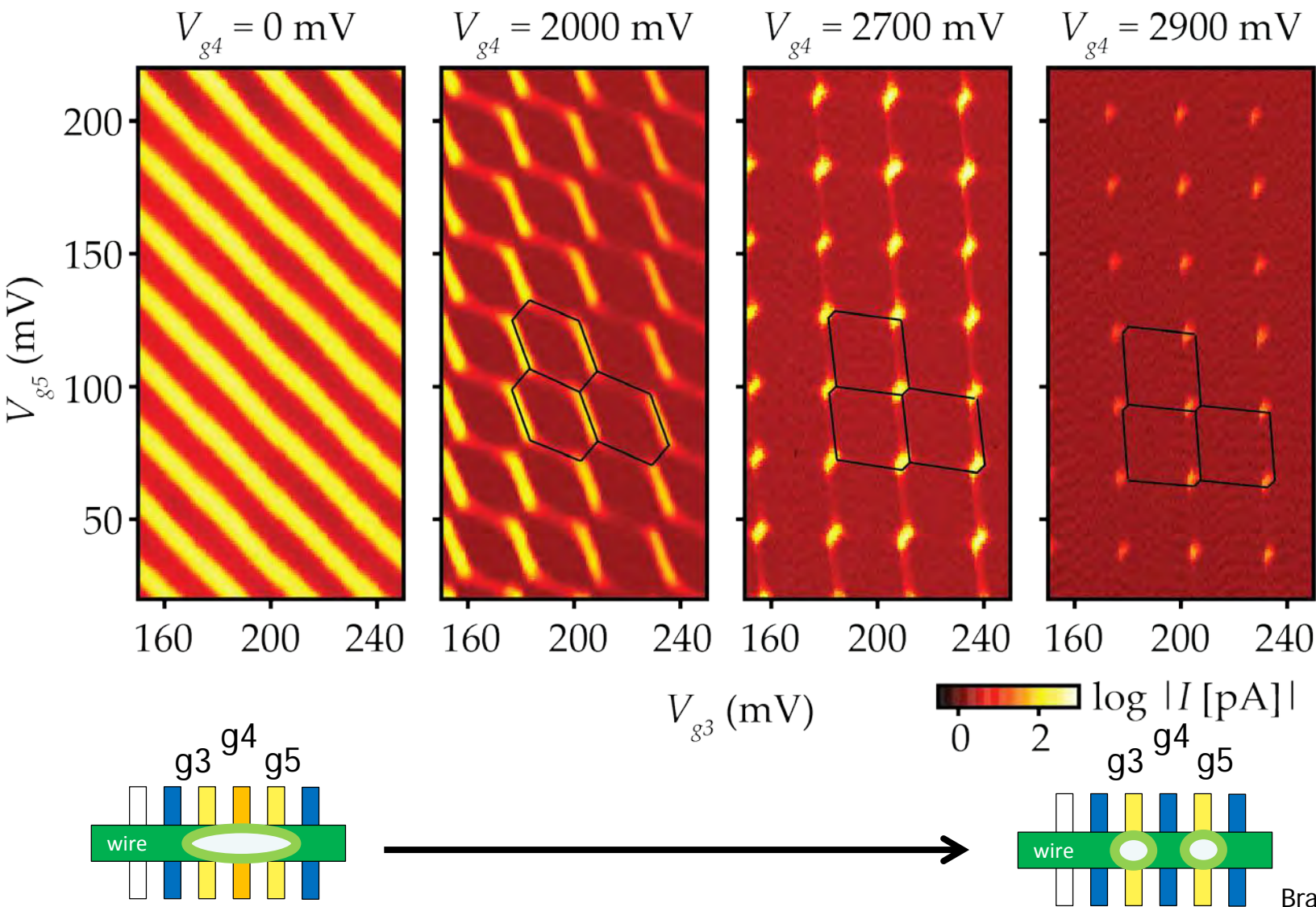
GE/SI CORE/SHELL NANOWIRES

- 0.5 micron long QD
- 30h measurement, few switches
- $N \sim 160$



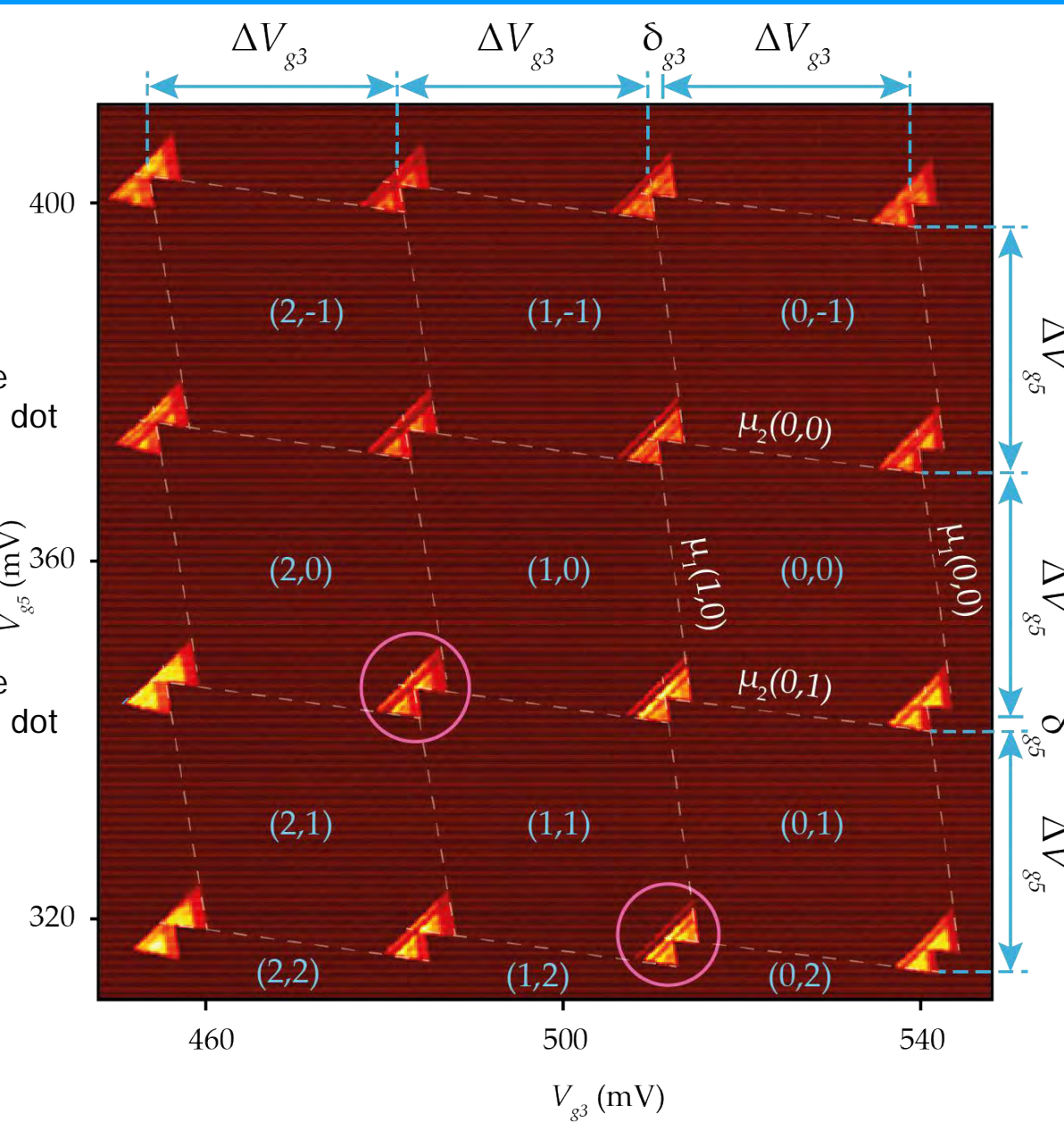
Ang Li et al, in review at Nature Comm

GE/SI CORE/SHELL NANOWIRES



GE/SI CORE/SHELL NANOWIRES

+1 hole to right dot
+1 hole to right dot



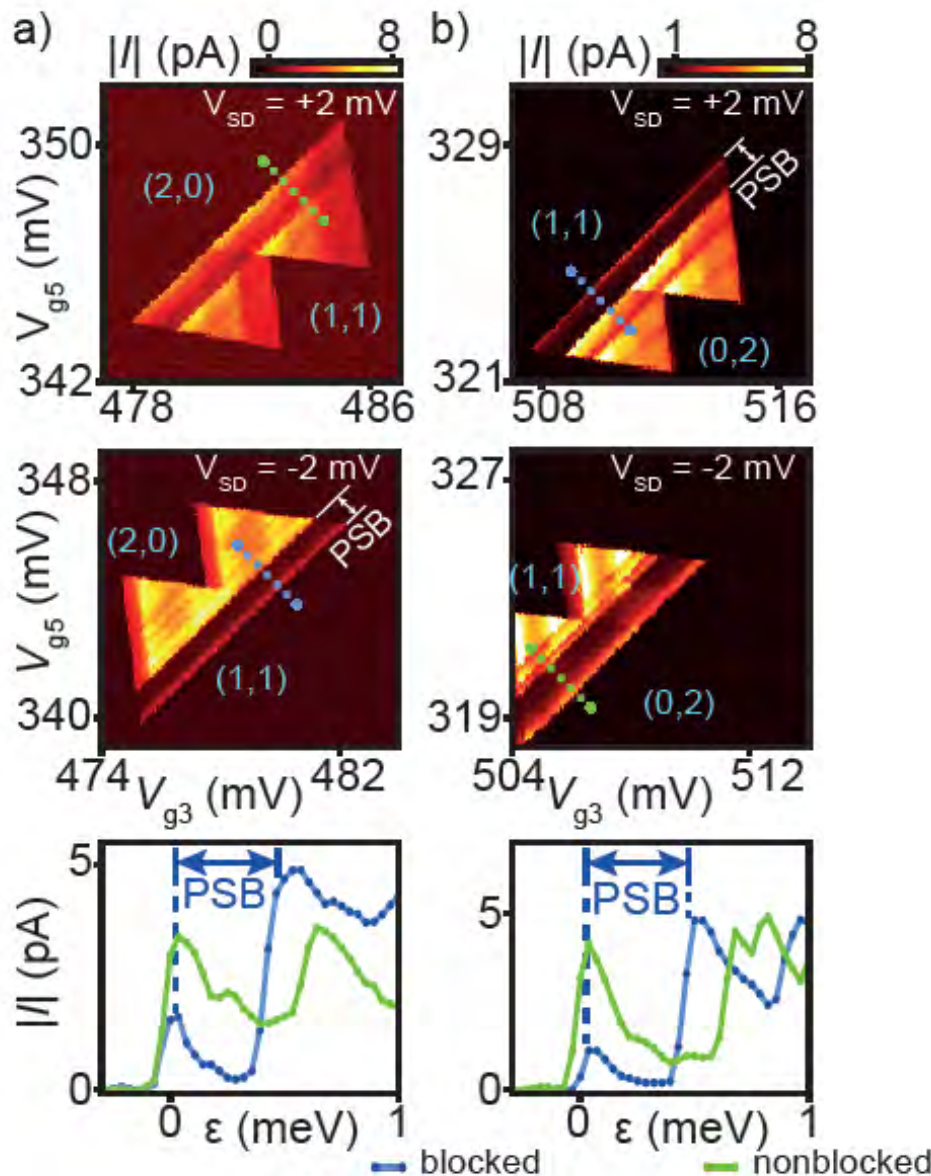
Shell filling in DQDs

$(n,m) \sim (70,70)$

$E_c \sim 10$ meV
 $E_{orb} \sim 0.6$ meV

Brauns et al, in review

GE/SI CORE/SHELL NANOWIRES



Pauli spin blockade

- at (1,1)-(0,2) at pos Vsd
- at (1,1)-(2,0) at neg Vsd

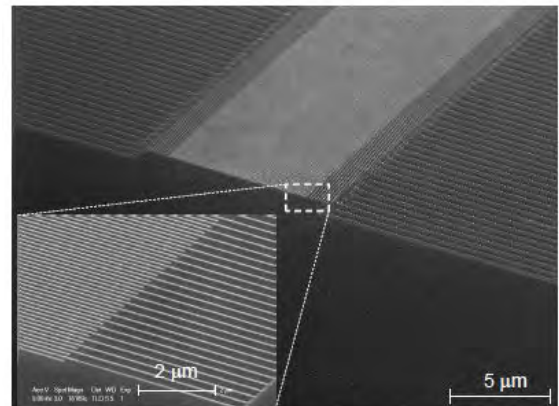
Hole spin blockade:

- Pribiag et al., Nat nano 2013
Li et al., Nano Lett 2015
Brauns et al., in review

Summary

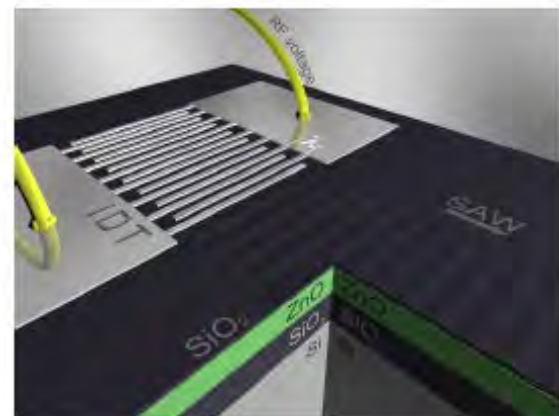
S. Büyükköse, B. Vratzov, D. Atac, J. van der Veen, P. V. Santos and WGvdW, Nanotechnology **23**, 315303 (2012).

ZnO/SiO₂/Si multilayer: max. 16 GHz



S. Büyükköse, B. Vratzov, J. van der Veen, P. V. Santos and WGvdW
Appl. Phys. Lett. **102**, 013112 (2013).

SiO₂/ZnO/SiO₂/Si: 23 GHz



S. Büyükköse, A. Hernández-Mínguez, B. Vratzov, C. Somaschini, L. Geelhaar, H. Riechert, WGvdW and P. V. Santos, Nanotechnology **25**, 135204 (2014).

